Past, Present and Future of Aerial Robotic Manipulators

Anibal Ollero, *Fellow, IEEE,* Marco Tognon, *Member, IEEE,* Alejandro Suarez, *Member, IEEE,*
Dongjun Lee, *Member, IEEE,* and Antonio Franchi, *Senior member, IEEE*

Abstract—This paper analyzes the evolution and current trends in aerial robotic manipulation, comprising helicopters, conventional under-actuated multi-rotors and multi-directional thrust platforms equipped with a wide variety of robotic manipulators capable of physically interacting with the environment. It also covers cooperative aerial manipulation and interconnected actuated multi-body designs. The review is completed with developments in teleoperation, perception and planning. Finally, a new generation of aerial robotic manipulators is presented with our vision of the future.

Index Terms—Aerial Manipulation, Aerial Robots Physically Interacting with the Environment, Unmanned Aerial Vehicles

TABLE I: Generations of aerial robotic manipulators.

	1st **Gen.**	2nd **Gen.**	3rd **Gen.**
Platforms	Helicopters Quadrotors	Helicopters Multi-rotors	Multi-rotors: fully actuated, multibody
Arms	Few DoFs	6/7 DoFs Compliance	Dual arms Hyper-redundant
Navigation	Motion tracking system	Indoor beacons GPS	SLAM
Perception	No onboard motion tracking	Onboard with markers	Onboard without markers
Planning	No planning	Ground station Basic reaction	On-board Reactivity

I. INTRODUCTION

THE field of aerial robots physically interacting with the environment, and particularly AErial RObotic Manipulators (AEROMs), has experienced ten years of sustained growth. Diverse prototypes, functionalities and capabilities have been developed and evaluated in representative indoor and outdoor scenarios, demonstrating the possibility to successfully perform manipulation tasks while flying. The ability of aerial manipulators to quickly reach and operate in high altitude workspaces, along with the level of maturity reached in recent years, led to the application of this technology in areas like inspection and maintenance, reducing time, cost and risk for the human workers. In this sense, this paper aims at providing a broad perspective and analysis of the work done in aerial manipulation, possibly helping engineers interested in designing an aerial manipulation robot for a specific task.

Reviewing the main achievements in this field, it is possible to identify common features that allow defining the classification proposed in Table I. Figure 1 shows the evolution of aerial manipulator designs in the last decade, although early achievements can be also found in the 90s with the disc lifting mission at the International Aerial Robotics Competition.[1] The first generation of aerial manipulators consisted of conventional quadrotors capable of applying forces to a wall while keeping flight stability [1], grasping objects [2] and constructing cubic structures [3] with an embedded arm with few Degrees of

Freedom (DoFs). Less conventional designs started to appear: [4] presents the modeling and control of a ducted-fan miniature UAV interacting with the environment; a 6 DoFs gantry crane equipped with two 4 DoFs manipulators was also proposed in [5]; and a three-active-DoFs delta-like manipulator with a three-passive-DoFs end-effector installed on a quadrotor was developed in [6]. These prototypes employed motion tracking systems for positioning in indoors [7]–[10], without relevant perception and planning.

Helicopters played an important role in the development of the aerial manipulation with early works in outdoors applied to load transportation [11]–[13], interaction with the environment [14], [15], and manipulation [16]–[18], showing better performance than multi-rotors in terms of payload capacity and operation time. However, the use of multi-rotors spread in following years because the control, mechanical construction and handling of these platforms are significantly simpler, and allow to mitigate safety problems associated to the blades of the helicopters main rotor.

The second generation includes adapted aerial platforms for both indoor and outdoor operations, equipped with rigid and compliant arms (up to 6/7 DoFs) for precise end-effector positioning and compensation of perturbations. They also integrate outdoor navigation sensors based on GNSS (Global Navigation Satellite System), indoor navigation features based on beacons, on-board perception with markers, and off-board planning features. Outdoor experiments involving grasping with 7 DoFs arms with both helicopters [19] and multi-rotors [20] were presented. Different arm designs have been introduced as well, including parallel manipulators with a large singularity-free workspace [21] for precise end-effector positioning relative to a target [22], or a hyper-redundant manipulator for mobile manipulating UAVs [23]. Attention was also paid to control techniques validated in simulation [24]. In [25] a framework for outdoor aerial manipulation is presented. Regarding vision-

A. Ollero and A. Suarez are with the GRVC Robotics Lab, Universidad de Sevilla, 41012 Sevilla,Spain. E-mail: aollero@us.es (see https://grvc.us.es)

M. Tognon is with the Autonomous Systems Lab, ETH Zurich, 8092 Zürich, Switzerland. E-mail: mtognon@ethz.ch

D. Lee is with the Department of Mechanical Engineering, IAMD and IER, Seoul National University, Republic of Korea. e-mail djlee@snu.ac.kr

A. Franchi is with the Robotics and Mechatronics lab, EEMCS Faculty, University of Twente, Enschede, The Netherlands and with LAAS-CNRS, Université de Toulouse, CNRS, Toulouse, France. e-mail: a.franchi@utwente.nl

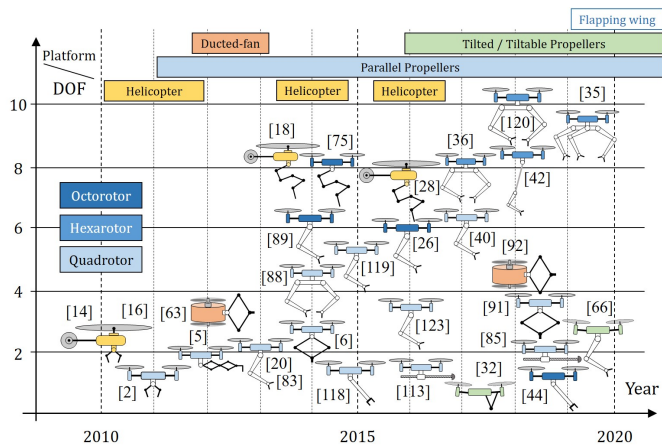[1]http://www.aerialroboticscompetition.org/mission1.php

Fig. 1: Evolution in the development of aerial manipulation prototypes, comprising different platforms and morphologies.

based controllers, a hybrid visual servoing with a hierarchical task-composition control is presented in [26]. An integrated vision-based guiding system for aerial manipulation with a stereo camera is shown in [27].

The current third generation of aerial manipulators includes several advanced features: operations in both outdoor/indoor environments [28], fully actuated platforms [29]–[32], multiple arms [33]–[36], GNSS free navigation capabilities, onboard SLAM [37], [38], on-board perception without markers [39], [40], off-board real-time planning with control awareness [41], [42], and on-board reactivity and planning. Applications include structure assembly, contact-based inspection in refineries (pipes and tanks) and bridges [43], [44].

The kinematics, dynamics and control of AEROMs with conventional multi-rotor platforms is shown in [33]. Significant similarities can be established with space [45] and underwater [46], [47] manipulation in the formulation and derivation of the kinematic and dynamic models. The use of dual arm systems in aerial and space manipulation was motivated by the convenience of partially compensating reaction wrenches induced over the floating base due to the motion of the operating arm. We notice that the gravity effect is probably the most limiting factor in an aerial manipulation robot in terms of payload capacity and operation time [11], [48]. An analogy can be also drawn between the aerodynamic [49] and hydrodynamic [46] modelling in aerial and underwater manipulators. Previous surveys on modeling and control of multi-rotor vehicles [54] and aerial manipulators [50], [51], provide a very good baseline for this paper. Here we extend them considering novel and more complex aerial platforms like flapping wing [52], [53], focusing not only on modeling and control methods, but also on teleoperation, perception, and motion planning techniques.

II. PLATFORMS FOR AERIAL MANIPULATION

Here we introduce the spectrum of different platform designs that can be used for aerial manipulation. It includes helicopter, ducted-fan and the most popular multi-rotor platforms. In our review, we group platforms by *types*, *i.e.*,

clusters defined according to major design characteristics. The platforms will be additionally clustered according to the actuation property, type of interaction tool, and performed tasks. We also review the popular control algorithms used to stabilize and steer these systems during physical interaction.

A. Modeling & Actuation Properties

Here we consider a rather general definition of *multi-rotor platforms* with a main body equipped with $n \in \mathbb{N}_{>0}$ actuators consisting of a motor-propeller pair that produces a thrust and a drag moment on the main body. Their intensities are proportional to the square of the propeller spinning velocity, $u_{\lambda_i} = |w_i| w_i \in \mathbb{R}$ [54]. We gather all control inputs relative to the thrust intensity in $\boldsymbol{u}_\lambda \in \mathbb{R}^n$. With respect to (w.r.t.) the body frame $\mathcal{B}$ attached to the main body, each propeller can be i) *rigidly fixed*, ii) *tiltable* by $m \leq 2n$ servomotors where $\boldsymbol{u_V} \in \mathbb{R}^m$ gathers their angular positions controlling the orientation of the propeller spinning axes, iii) *movable* by $r \leq 3n$ servomotors where $\boldsymbol{u_P} \in \mathbb{R}^r$ gathers their angular positions controlling the position of the propellers.

The dynamics of a generic multi-rotor is computed in [54]. One important element is the *full allocation matrix*, $\boldsymbol{F}(\boldsymbol{u}_\lambda, \boldsymbol{u_V}, \boldsymbol{u_P}) \in \mathbb{R}^{6 \times (n+m+r)}$. It defines how an input variation affects the total wrench generated by the platform. In [54], the analysis of $\boldsymbol{F}$ brought to the definition of actuation properties that characterize the set of feasible wrenches:

1) Uni-Directionnal Thrust (UDT): platforms with this property can vary the total thrust along one direction only (like in coplanar/parallel designs , helicopters and ducted-fans). We say that a platform is UDT if rank$\{\boldsymbol{F}\} = 4$. For helicopters and ducted-fan vehicles, the previous model does not apply directly. In general, the total thrust and torque are considered as inputs [16], [18]. Since the direction of thrust is constant w.r.t. body frame, the corresponding allocation matrix has rank 4, which makes such vehicles UDT.

2) Multi-Directionnal Thrust (MDT): platforms with this property can vary the total thrust along more than one direction independently from the total moment. We say that a platform is MDT if $5 \leq$ rank$\{\boldsymbol{F}\} \leq 6$.

3) Fully Actuated (FA): this describes a sub-class of MDT platforms. Platforms with this property can vary the total thrust along all directions independently from the total moment. We say that a platform is FA if rank$\{\boldsymbol{F}\} = 6$.

4) Over Actuated (OA): with this property we describe multi-rotor platforms that are FA and have more actuation inputs, $n_u = n + m + r$, than degrees of freedom. A multi-rotor is OA if it is FA and for each desired wrench there is more than one input combination that realizes it, *i.e.*, $n_u > 6$.

5) Omni Directional (OD): this describes another sub-class of FA designs, not exclusive from OA, where the total thrust can assume any value in a spherical shell independently from the total moment. A more detailed study on the theoretical characterization of OD multi-rotors with unidirectional propellers is provided in [31].

B. Control Methods for Contactless Tasks

If the platform is FA, the design of the controller is rather straightforward because the full allocation matrix $\boldsymbol{F}$

is invertible. This allows applying simple *static* (for fixed propellers) or *dynamic* (for tiltable and movable propellers) *feedback linearization* that allows the independent control of the position and orientation [55]. If the platform is OA, the null space of $\boldsymbol{F}$ can be used to optimize the control inputs [56].

If the platform is not FA, feedback linearization cannot be directly applied. A specific controller should be designed to face the underactuation. For quadrotors and helicopters, to apply dynamic feedback linearization a first input transformation is required considering the total thrust and moment as input.

Feedback linearizable systems are also differentially-flat [57]. It follows that any FA vehicles is differentially-flat w.r.t. position and orientation. Additionally, it has been proven that UDT vehicles, like quadrotors, ducted-fan and helicopters, are also differentially-flat w.r.t. center-of-mass position and yaw angle. Therefore, every UDT and FA (as well as OA and OD) aerial platforms are differentially-flat, although with different flat outputs. Differential-flatness based controllers can be used to control the robot position in contactless tasks.

The dynamics of the position of the center of mass of the full AEROM is decoupled from the orientational and postural dynamics, and it resembles the one of a UDT vehicle [58]. Therefore, AEROMs are differentially-flat systems with the global-center-of-mass position as flat output [59]. However, the end-effector position – the most relevant output for contact-based operations – is part of a flat output only for specific design of AEROMs [60], [61].

Other general methods that can be applied independently to FA and non-FA platforms are based on *Model Predictive Control* (MPC). In [62], a nonlinear MPC-based controller which considers the full nonlinear dynamics of the system and inputs constraints is proposed for any multi-rotor. However, a precise model of the system is required, as well as a fine tuning of the cost function. In practice, according to the complexity of the system, both requirements could be difficult to be obtained. In such cases, feedback linearization can be simpler to implement, especially in the static case.

C. Control Methods for Aerial Physical Interaction

When aerial vehicles are in interaction with the environment, they need to be able to control at the same time the position at the contact, and the interaction force, preserving the stability of the entire system. In the following we review the most common control techniques designed for this scope.

1) Impedance/admittance control: this is probably the most common approach based on the re-shaping of the impedance/admittance mechanical properties of the system at the interaction point. Impedance/admittance controllers establish a desired dynamical relationship between the end-effector position and the interaction force.

The *impedance control*, treats the system as a mechanical admittance. The input of the system is the force actuated by the robot and the output is the displacement of the end-effector. In practice, to perform contact-based tasks, the desired position of the end-effector is chosen 'inside' the surface of interaction. The robot, trying to reach this point will generate a force that is related to the impedance properties of the controller. Such

strategy has been proposed for both underactuated and fully-actuated aerial manipulators [63]–[68]. Notice that the compliance of the robot can be designed both software or hardware, by the controller or a suitable mechanical design [66], [69].

The *admittance control* is the dual of the impedance control. It treats the system as a mechanical impedance. The input of the system is the displacement of the end-effector and the output is the interaction force. Such strategy has been proposed for both underactuated and fully-actuated aerial manipulators [32], [70]–[75].

Passivity-based and *Port-Hamiltonian methods* have been also employed to design similar approaches which aim at the reshaping of the apparent impedance/admittance properties of the system [76], [77].

2) Hybrid position/force control: previous schemes implement an indirect force control where the interaction force is indirectly controlled by designing a suitable end-effector trajectory. On the other hand, the hybrid position/force control method aims at precisely controlling the interaction force in a direct way. The robot is controlled by two complementary feedback loops, one for the position, the other for the interaction force, along the unconstrained and constrained axes, respectively. Such a control strategy has been implemented for UDT [60], [78]–[80], and FA [81] vehicles. In [82] a direct force-controller based on optimization is presented.

In order to implement the previously presented controllers, the estimation of the state (addressed in Section VII-B) and interaction forces are needed. For the latter, model-based wrench observers like the ones in [32], [76], can be employed. A more direct solution is the use of a force sensor attached to the end-effector [70], [82]. This allows to implement a direct feedback in the interaction control loop.

We note that impedance/admittance controllers are very easy and intuitive to implement. Furthermore, the transition from contactless and contact-based flight can be easily handled with a smooth variation of the gains. However, precise interaction control is not guaranteed. On the other hand, hybrid position/force controllers can provide accurate position and force tracking but contact constraints have to be carefully addressed.

D. Physical Interaction Tasks

Here, we classify the physical interaction tasks addressed by the aerial robotic community. In particular, we consider only tasks that involve an exchange of forces (or moments) between the environment and the aerial robot.

1) Pick & Place (P&P): the objective is to grasp or release an object not constrained to the environment [36], [75], [83], [84]. The interaction forces play a role only during the pick and place operations, which are normally very short in time and can be considered negligible in most of the cases.

2) Point contact (PC): the objective is to preserve the contact between the environment and the robot end-effector in a single static point. If the end-effector position is constrained, the challenge is to control the intensity and direction of the interaction force [80]. On the other hand, if the end-effector is free to move, the challenges are multiple: i) Manage the transition from contact-free to contact flight, namely from

zero to non-zero interaction forces. Bouncing effects or strong impacts could destabilize or damage the robot; ii) Ensure a sufficient force normal to the interacting surface to guarantee the contact; iii) Keep the interaction force in the friction cone. If this is not ensured, the end-effector might slip causing the crash of the robot. Applications falling into this category are the installation of sensor devices [85], the inspection by contact of tanks [44], pipes [66] and other surfaces [6], [86].

3) Pulling/pushing (PP): this task is similar to the contact point, but the point of interaction is non static. The interacting surface is not fully constrained and can move in the space along certain directions. When the robot is asked to pull an object, the end-effector position (and perhaps orientation) is in general constrained to the point of interaction. On the other hand, when the robot is asked to push an object, the mechanical constraint between the end-effector and the object is not required as long as the interaction force lays in the friction cone. For pulling/pushing tasks, the extra challenge w.r.t. point contact is the dynamics of the object that now needs to be considered, together with its kinematic constraints. Classical benchmarks consist of opening/closing a drawer or a door and pulling/pushing a cart.

4) Sliding (S): the objective is to keep the contact between the end-effector and a static surface, while the end-effector moves on it. The static and dynamic frictions must be considered in the control problem to avoid slippage, ensure the contact, and move the end-effector along the desired trajectory. The most popular application is the continuous contact-based inspection of tanks [44], pipes [66] and other surfaces [87].

5) Peg-in-hole (PH): the objective is to insert an object (attached to the end-effector) in a hole. If the difference in size between the object and the hole is small, this operation can become very difficult. During the insertion, many of the DoF of the end-effector are constrained. This requires both a precise knowledge of the environment and a suitable impedance shaping to cope with errors and uncertainties that are present in real applications. If impedance shaping is not carefully addressed, high-frequency vibration and resonant effects could lead to instability or damages of the robot.

6) Manipulation (M): under this last category, we gather all such operations that require the application of specific forces and torques. Examples are the bending of a pipe or a bar, the opening/closing of a valve [88], assembly of structures [89], tree cavity inspection [90], or corrosion repair [91].

According to the specific physical interaction task, aerial platforms are equipped with different tools. The most common are: *rigid link (RL)*, a link rigidly attached to the robot; *gripper (GR)*; *passive links (PL)*, similar to rigid links, but attached to the vehicle by a passive joint (e.g., cables); *Articulated arm (AA)* (see Section III). Some times, the end-effector is made of a soft material, or includes a spring mechanism [6], [44], [66]. This makes the end-effector naturally compliant with the environment from a mechanical point of view.

E. Types of Multi-rotor Platforms

We finally review all the multi-rotor platforms that have been employed for physical interaction. We gathered them

TABLE II: Multi-rotor platforms for physical interaction tasks.

Platform	Actuation property	Interac. tool	Task	Reference	Maturity
HL	UDT	GR	P&P	[16], [17]	Exp.
		AA	M	[18]	Exp.
DF	UDT	RL	PC	[64]	Sim.
		AA	PC	[92]	Exp.
ParP	UDT	RL	PC	[93]	Exp.
			S	[76], [94]	Exp.
		GR	P&P	[2]	Exp.
		PL	Transp.	[13], [95]–[97]	Exp.
			P&P	[98]	Exp.
			PC	[79]	Exp.
			M	[99]	Exp.
		AA	see Section III		
TedP	FA	RL	PC S PH	[32], [77] [32]	Exp.
		PL and GR	P&P M	[100], [101]	Exp.
		AA	PC S	[66], [82]	Exp.
	OA	RL	PC	[102]	Sim.
		AA	S	[44]	Exp.
	OD	RL	push S PH	[81]	Exp.
		GR	P&P	[29]	Exp.
TableP	MDT	PL	PC	[103]	Exp.
	OD and OA	RL	S	[86], [87]	Exp.
M	-	-	P&P	[104], [105]	Exp.
	-	-	PP	[106]	Exp.
MP (DF)		RL	PC	[107]	Exp.
MP (ParP)	-	PL	M	[108]	Exp.
MP (TedP)		PL	M	[109]	Exp.

into clusters sharing similar design characteristics related to the actuation (see Table II). For completeness, we also include helicopters and ducted-fan platforms which have been investigated in the early state of aerial manipulation. Figure 2 shows an example for every type of platforms. Exploiting the previous discussion, we also mention the actuation properties, the employed actuation tools, and the targeted tasks.

1) Helicopter (HL): consists of a main horizontal rotor, providing vertical lift, and a tail rotor mounted vertically to counteract the torque from the main rotor. This type of actuation makes helicopters UDT. Despite this, helicopters were one of the first platforms employed for aerial manipulation. The high payload allowed to equip them with cables for transportation [12], [13], with a gripper for pick & place [16], and with industrial robotic arms for manipulation [18], [110]. However, helicopters do not seem a really viable option in many applications due to their high complexity and danger during flight close to surfaces. Likely this is the reason why recent works are rather focused on multi-rotor platforms. In [111] an helicopter is considered but for the sole objective of holding a cable suspended multi-rotor aerial manipulator.

2) Ducted-fan (DF): consists of a main propeller mounted within a cylindrical duct together with some control surfaces. The first creates the total thrust, while the seconds generate moments to control the vehicle attitude. In view of this, it is easy to verify that standard ducted-fan platforms are UDT. In [63] a ducted-fan equipped with a simple rigid tool has been

(a) Helicopter [18]. (b) Ducted-fan [92]. (c) parallel- prop. [93].

(d) Tilted-prop. FA [82]. (e) Tilted-prop. OA [44]. (f) Tilted-prop. OD [29].

(g) Tiltable-prop. OD [86]. (h) Morphing UDT [105]. (i) Multi-platform sys. [108].
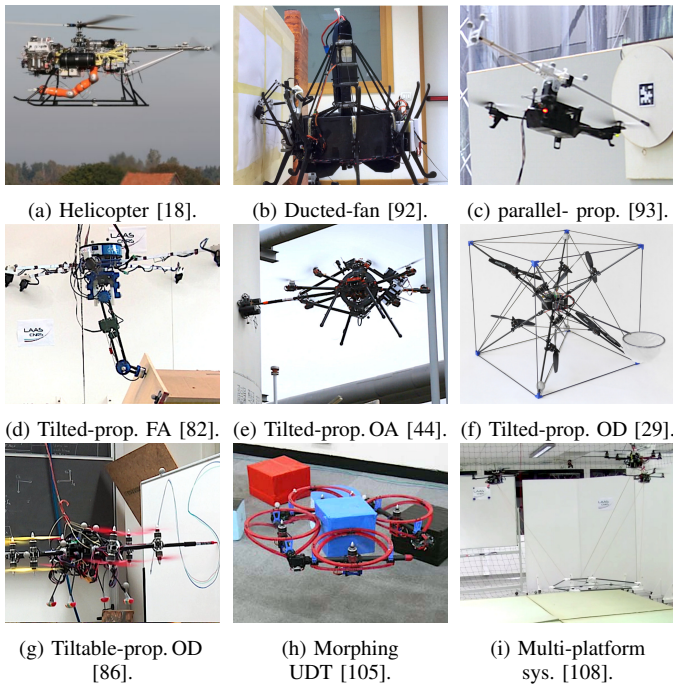
Fig. 2: A representative example for each type of multi-rotor platforms employed for physical interaction.

considered for contact point tasks in a simulation environment. Later, in [92], a real platform equipped with a parallel Delta arm has been experimentally validated for contact point tasks.

3) Parallel-propellers (ParP): consists of a main rigid frame equipped with multiple propellers fixed to the main frame. Every propeller is directed toward the same direction and typically arranged on the same plane. In the most common cases, they are characterized by four, six, or eight propellers, thus commonly called *quadrotor*, *hexarotor*, *octorotor*.

In the market, as well as in the state of the art related to aerial physical interaction, this type of platform is the most common. To perform physical interaction tasks, parallel-propellers platforms have been equipped with:

• *rigid links*, for point contact [93] and sliding tasks [76], [94];
• *grippers*, for pick & place operations [2];
• *passive links*, and in particular cables for transportation [13], [95]–[97], pick & place [98], point contact [78], [79] and manipulation (assembly) [99];
• *articulated arms*, for a wide range of tasks, e.g., pick & place [112], point contact [113], pulling/pushing [114], sliding, and manipulation [88]. A complete review is given in Section III.

4) Tilted-propellers (TedP): consists of a main rigid frame equipped with multiple propellers fixed to it. The propellers are directed toward multiple directions. According to the number, orientation, and type (unidirectional/bidirectional) of propellers, such platforms can be FA, OA, or even OD.

Among the FA platforms, we find the "TiltHex" [55] which has six unidirectional-propellers rigidly attached to the main body, and oriented in different directions. Such a platform has been equipped with i) a rigid tool for point contact [77],

slide, and peg-in hole tasks [32]; ii) a passive link together with a gripper for pick & place and manipulation tasks [100], [101]; iii) an articulated arm for point contact and slide tasks [66], [82]. Among the OA platforms (non OD) we find the "AEROX" [44] which has eight unidirectional-propellers rigidly attached to the main body, and oriented in different directions. This platform has been equipped with an articulated arm for point contact and slide tasks and has been applied for contact inspection of both oil and gas plants and bridges [43]. Among the OD platformss we can find "ODAR" [81] which has eight bidirectional-propellers rigidly attached to the main body, and oriented in different directions. Such a platform has been equipped with a simple rigid tool for tasks like push and slide and peg-in-hole. A platform with a similar propellers configuration is the one in [29]. The platform has been equipped with a pouch for pick & place operations and it has been used for the dynamic catching of a thrown ball.

5) Tiltable-propellers (TableP): consists of a main rigid frame and multiple propellers fixed to movable actuated elements (servo motors). Thanks to the extra actuation, the propellers can be directed toward multiple directions in an independent or coordinated way according to the specific actuation configuration. Several designs have been presented with a different number of tiltable propellers going from 2 to 8, except for 5 and 7. Some of these platform have been proposed in [30], [56], [103]. For a detailed survey on platform with tiltable-propeller, we refer the interested reader to [54]. Although most of the tiltable-propellers platforms are at least FA, there are only few cases in which they are used for physical interaction. In fact, the servo motors are in general not very precise and have a slow dynamics, as well as additional mechanical issues as backlashes.

In [103], the authors propose a tri-rotor platform in a "T"-like configuration, where the two frontal principal propellers can tilt radially by the same angle, while the tail rotor can tilt independently. Such actuation configuration makes the platform MDT. The platform has been equipped with a passive 1-DoF revolute end-effector to accomplish point-contact tasks. In [86], [87], the authors propose a twelve-rotor platform in a double motor configuration, where each pair of propellers can tilt radially. Such actuation configuration makes the platform OD and OA. The platform, equipped with a rigid tool has been used for point contact and sliding tasks.

6) Multi-rotor Morphing (M): consists of a main body composed by actuated links. Each link, or part of them, is then equipped with one (or multiple) tilted- or tiltable-propellers. Thanks to the actuation of the main body links, the robot can not only change the propeller directions, but also their relative positions. Although the mechanical design is even more complex than TableP platforms, morphing ones allow for a very high adaptability to the environment and task needs.

In [115] a quadrotor-like platform with foldable arms has been proposed for simple contactless navigation purposes. For similar tasks, e.g., passing through narrows gaps, a transformable multi-linked aerial robot has been presented in [116].

Again, likely due to the mechanical and control complexity of such platforms, M-type aerial systems physically interacting with the environment have been rarely presented. One example
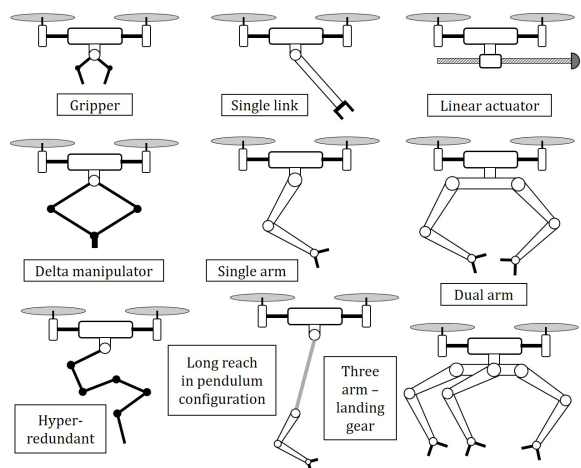
Fig. 3: Different morphologies of aerial manipulation robots.

TABLE III: Different prototypes of manipulators, sorted by number of DoFs. Types of platforms are Multirotor (M) and Helicopter (H). Manipulators are: Stiff (S), Compliant (C), and Industrial (I).

Morpho.	Ref	Type	DoF	Reach	Weight	Payload
Gripper	[2]	M-C	1	-	-	-
	[16]	H-C	2×4	0.39	-	1.5
Single	[118]	M-C	1	-	-	-
link	[87]	M-S	0	-	-	-
	[44]	M-C	1	-	-	-
Linear	[113]	M-C	1	-	-	-
actuator	[85]	M-S	1	0.4	0.48	4.5
Delta	[6]	M-C	3	0.2	0.22	-
manip.	[21]	M-S	3	0.36	0.5	-
	[91]	M-S	3	0.25	0.22	-
Single	[83]	M-S	2	0.32	0.37	-
arm	[20]	M-S	2	-	0.4	0.2
	[66]	M-S	2	-	-	-
	[119]	M-S	5	0.3	0.25	0.2
	[89]	M-S	6	0.45	1.4	-
Multi	[88]	M-S	2×2	-	-	-
arm	[36]	M-C	2×4	0.5	1.3	0.3
	[120]	M-S	2×5	0.5	1.8	0.7
	[35]	M-C	3×3	0.37	1.0	-
Hyper-	[19]	H-I	7	0.88	22	7
Redundant	[75]	M-S	7	-	-	-
Long	[121]	M-C	$2 + 1$	1.5	0.8	0.2
reach	[34]	M-C	$8 + 1$	1.5	1.6	0.3

of the M-type that has been used for physical interaction is the "HYDRUS" [105]. It consist of a two-dimensional multi-link structure, where each link is equipped with a propeller. The robot exploits its morphing capability for pick & place operations. It can grasp objects of different shapes properly adapting its configuration [104]. An evolution of such a vehicle used for manipulation tasks has been presented in [106], [117].

7) Multi-platform systems (MP): consists of multiple multi-rotor platform (belonging to the previously described types) physically connected forming a new articulated flying platform. Examples of such multi-rotor based platforms are actuated by: 1) ducted-fans [107] for point contact tasks, 2) parallel-propellers platforms [108] for manipulation tasks, 3) tilted-propellers platforms [109] for manipulation tasks. This particular case of multi-robot cooperation for aerial physical interaction is addressed in detail in Sec. IV.

III. AERIAL PLATFORMS WITH ROBOTIC ARMS

A. Morphologies of Aerial Manipulation Robots

The literature review in aerial robotic manipulation reveals a wide diversity of morphologies mainly differing from the designs and implementations of the manipulator, using autonomous helicopters [17], [18] and multi-rotors [20], [83] as aerial platforms. The analysis and comparison of the prototypes according to their kinematic configuration, functionalities, and mechanical construction allows the classification reported in Figure 3 and Table III.

Possibly because of the widespread use of industrial robotic arms, a significant number of aerial manipulation prototypes employ an upper arm-forearm configuration including shoulder, elbow, and wrist joints, both in the single arm [83], [89], [119] and dual arm [120] case. The number of joints and the kinematic configuration of the arms are determined in principle by the level of dexterity required in the manipulation task, minimizing the number of actuators to reduce the total weight. Redundant and hyper-redundant manipulators [19], [23], [66] are intended to perform tasks requiring the appropriate positioning and orientation of the end effector when interacting with the objects or the environment. In order to reduce the reaction wrenches induced by the motion of the manipulator,

some prototypes employ transmission mechanisms like timing pulleys [118], [119], or rigid bars [120], placing the actuators as close as possible to the base of the aerial platform. The use of parallel mechanisms, as in delta manipulators [6], [21], [91], is useful to reduce the inertia, however the workspace range is typically much lower compared to a serial manipulator arm. Aerial manipulators with single link [44], [87], [118] and linear actuators [85], [113] have been proposed for tasks involving force interactions with surfaces [93].

The technological limitations of the servo actuators typically employed for building lightweight robotic arms [75], [89], [119], [120], [122], whose capabilities are usually limited to position/velocity control, impede the realization of manipulation tasks involving significant interaction forces. To overcome this problem, the works in [70], [82] employ a F/T sensor attached at the wrist of a stiff-joint manipulator. Alternatively, in [36], [69], [76], [123] the estimation and control of the torques acting over the servos is done by measuring the deflection of an elastic element introduced between the actuator and the output link. The works in [85], [113] exploit the kinetic energy of the aerial platform to apply higher forces, using a linear actuator to regulate the impact force interaction in a passive [113] or active [85] way.

Motivated by the convenience to increase the separation distance between the manipulator and the propellers, the concept of long reach aerial manipulator with dual arm is introduced in [124]. Later, this morphology evolved to the concept of aerial manipulator in pendulum configuration with passive joint at the base [121] [42], increasing safety in the realization of manipulation tasks close to environmental obstacles [34].

B. Compliance

The term compliance in robotic manipulation can be defined as the manipulator ability of accommodating for the forces

generated during the physical interactions with the environment or with an agent (human or robot). Intuitively, this concept is associated to an elastic behavior in the joints or links. More formally, the compliance can be formulated as the mechanical impedance (or, analogously, the admittance) that relates the position deviation of the manipulator with the external force, characterized by the inertia, damping, and stiffness. Two forms of compliance can be identified depending on its physical realizations: mechanical [15], [113], [118], [123], [125], or at control/software level [69], [70], [85]. In the first case, an elastic element is introduced in the joints or links of the manipulator, such that a significant deformation is produced when a force within the nominal range of the actuators is exerted. On the other hand, most industrial robotic arms like KUKA, Universal Robots or ABB, integrate accurate force/torque sensors to control the apparent impedance.

The compliance is a highly desirable feature for an AEROM physically interacting with the environment since the stability of the floating base may be compromised by the forces caused by the dynamic coupling with the manipulator. The ability of accommodating for the motion of the aerial platform [64], [71], [77] and/or the manipulator [69], [76], [113] results very convenient when considering the uncertainties associated to the in-flight operations, especially in outdoor scenarios.

The first works that introduced compliance in aerial manipulation [16], [113], [118], [123], [125] proposed different compliant mechanisms designed for their integration in helicopters and multi-rotors, like grippers [16], lightweight robotic arms [36], [123], linear actuators [113], or flexible joints [118]. Several functionalities were demonstrated, including collision detection and reaction with active-passive compliance [123], [125], generation of high impact forces [113], deflection based torque/force control [69], and safe interaction in contact with the environment [76]. The anthropomorphic, compliant and lightweight dual arm presented in [36] combines the mechanical compliance with servo protection to improve the robustness, preventing that the actuators are damaged due to impacts or overloads. The modeling and control of compliant joint/arms was extended in [69], proposing a force controller based on Cartesian deflection. The passive joint in the long-reach (pendulum) configurations [34], [42], [121] provides an enhanced capability of accommodation thanks to the fact that no torque is transmitted to the aerial platform about the joint axis, while the force is still exerted along the link direction. In case of impact, the energy absorbed is stored as potential energy in the pendulum, and released later as kinetic energy.

C. Design and Mechatronic Aspects

Although the manipulator should provide a sufficient level of dexterity to accomplish the task, increasing the number of joints of the manipulator introduces some problems. The most evident is the reduction in the payload capacity and flight time of the aerial platform. This can be clearly identified expressing the mass distribution of the AEROM as $m_{AP} + m_M + PL_M <= \eta MTOW$, where m_{AP} is the weight of the aerial platform (including all its components except the manipulator), m_M and PL_M are the weight and

payload capacity of the manipulator, $MTOW$ is the maximum take-off weight, and η is the load index of the platform. Different approaches can be adopted in the design of the robot depending on how this equation is interpreted:

• Design determined by the weight of the payload (PL_M): some works propose the use of aerial robots in tasks involving the grasping [36], [83], [84], installation [85] or interaction [44], [66] with devices whose weight is predefined.

• Design determined by the level of dexterity (m_M): the number of joints is designed to obtain the manipulation dexterity required to accomplish the task. It is possible to distinguish between manipulators that use the joints for end-effector positioning [20], [35], [66], [83] or orientation [19], [119]. Insertion [110] and assembly operations [89] are examples where joints for orienting the wrist are required.

• Design determined by the available payload ($MTOW$): if the user or application demand the use of a particular aerial platform, then the weight of the onboard systems (m_{AP} and m_M) and the payload capacity (PL_M) are constrained by $\eta MTOW$. For example, safety reasons may impose a maximum total weight or maximum size of the AEROM.

Metrics like the lift load capacity or the payload-to-weight ratio are useful for evaluation and comparison purposes [48]. The so called smart servos like Dynamixel [35], [83], [88], [89], [91] or Herkulex [36], [120] are currently the best option for building lightweight robotic arms for aerial manipulation. These devices integrate the motor, gearbox, electronics and communications in a compact device with a relatively high torque-to-weight ratio. These features significantly simplify the design and development tasks, although their performance is limited to position control at low update rates, usually below 100 [Hz]. Some models allow the open-loop torque control, acting directly over the current signal. However, the friction of the gearbox makes impossible to estimate or control accurately the torque at the output link.

D. Single Arm vs Dual Arm

Most of the aerial manipulation prototypes developed in the last decade consider a single manipulator attached to the aerial platform, and only a few of them explore the use of two [36], [68], [88], [120] or three [35] arms. By using identical arms, the integration on the platform is simplified and shoulder-like mechanical interfaces can be used to interconnect the arms with the platform, as in [36], [120].

The dexterity and manipulation capabilities of a dual arm system allow the realization of tasks that cannot be accomplished with a single manipulator. The grasping and manipulation of long objects like bars or tubes [42] is a clear example where a dual arm manipulator results more convenient than a single arm. Other examples are: valve turning [88], cooperative bimanual grasping, and some assembly operations [89]. A multi-arm system increases the payload capacity, extends the effective workspace of the aerial manipulator [120], [121], and allows the partial cancellation of the reaction wrenches induced by one arm over the aerial platform using the other arm as reaction [120]. The development of human-size [120]

and human-like [36] dual arms is also motivated by the convenience to replicate the abilities of human operators.

One capability of a dual arm aerial manipulator that results especially interesting is the use of one arm as position sensor relative to a grabbing point while the other arm conducts the manipulation task. The idea is to estimate the position of the aerial platform relative to the grabbing point from the information provided by the joint servos. It is necessary to remark that the positioning accuracy of the aerial platform should be below the 10% of the reach of the manipulator to ensure that the aerial manipulation task can be accomplished in a reliable way [48]. This problem is very relevant in outdoors applications, as the accuracy of position estimation systems like RTK-GPS may not be good enough.

E. Control

The functionalities and potential applications of an AEROM are determined by the control capabilities of the aerial platform and the manipulator, considered as a whole. In the following we revise specific motion controllers for aerial manipulators based on the dynamic model [43]:

• *Decoupled*. These methods consider the aerial vehicle and the robotic arm as two sub-systems that are controlled independently [65], [70], [122]. The decoupled approach relies on the assumption that the influence of the manipulator over the attitude and position dynamics of the aerial platform is relatively small. The dynamic coupling is neglected or at best treated as a disturbance to compensate [19]. This motivates the design of low weight and low inertia manipulators [119], [120]. Decoupled control methods best perform only in quasi-static motions. As soon as the motion is more demanding in terms of accelerations, these methods fail, or in the best case show large tracking errors.

• *Coupled*. These methods consider the system as a unique entity. The design of a coupled control scheme relies on the full dynamic model, which explicitly takes into account the dynamic coupling through the inertia matrix [120]. Therefore, this approach is more suited for dynamic cases and allow better performance in terms of position accuracy and stability. Coupled controllers proposed in the state of the art are strongly model-based and consider the full dynamics of the system [58], [61], [126]. A complete overview of such control methods is available in [51]. Furthermore, it requires the real-time computation of the dynamic model of a system with $6 + NM$ degrees of freedom, being N the number of arms and M the number of joints per arm. They often require torque controlled motors that are in general unfeasible for aerial manipulators built with conventional servo actuators.

• *Partially coupled*. The control of the aerial platform and the manipulator are independent, but the controllers exploit the information provided by each of the systems to estimate the interaction wrenches and improve the performance of the compound, typically in terms of positioning accuracy [75], [83]. To this category belongs the multi-layer architecture presented in [122], where a momentum-based observer [71] is employed to compensate the dynamic couplings, and the variable parameter integral backstepping controller in [20].

• *Decoupled flatness-based*. This approach is in between decoupled and coupled approaches. Each degree of freedom is controlled independently, as in a decoupled controller, but the full system dynamics is considered via a feed-forward term computed thanks to the differential flatness property of some aerial manipulators [127].

F. Design and Application Guidelines

Given the wide variety of prototypes that can be found in the literature, it is convenient to formulate a design methodology to facilitate the development of specific solutions to particular applications. Autonomous helicopters are in general more suited for the manipulation of heavy loads and high operation times. Fully actuated multi-rotors equipped with few DOF's manipulators are suitable for exerting contact forces on surfaces like walls or tanks, whereas dexterous robotic arms are more appropriate when the application requires the adequate full-pose control of the end-effector. Delta manipulators have been employed due to their compact design and low inertia, that favors the accurate position control. Dual arm and three-arm systems have been proposed to conduct bi-manual manipulation tasks where a single arm may not be appropriate, introducing the long reach configuration to improve safety by reducing the probability of collision.

The design and development of an aerial manipulation robot requires the choice of the specific components or modules required to accomplish the task in the most effective and reliable way, rather than developing a general purpose aerial robot. Some features like accurate position estimation and control or compliant interaction control are usual requirements in a wide variety of applications. The positioning accuracy is probably one of the most challenging requirements in outdoor scenarios. Nevertheless, the operation time and payload capacity of the aerial platform, which are directly related to its size and weight, are currently the two main limiting factors in practice. The use of big platforms ($> 25\,[\mathrm{kg}]$ weight) should be avoided due to the inconveniences associated to its deployment and operation, safety, regulation, maintenance and repair.

IV. COOPERATIVE AERIAL MANIPULATION

To handle an object too heavy or too large for a single aerial robot, the concept of cooperative manipulation has been investigated. A team of multiple aerial robots is deployed to transport and manipulate a common object while increasing the total payload or the moment arm length via their cooperation. In this section, we survey some representative works in the area of cooperative aerial manipulation.

One of the earliest successful demonstrations for this aerial cooperative manipulation is the cable-suspended transportation and manipulation by multiple quadrotors or helicopters (e.g., [7]–[10], [12], [13], [108]). The works of [7]–[9] considered the problem of cooperative transportation of a triangular plate-like payload by three quadrotors with a cable connected between each of their center-of-mass and a point on the payload (see Figure 4). The key idea of [7], [8] was to convert the problem as a quasi-static motion planning problem, that is, given each waypoint of the desired payload pose
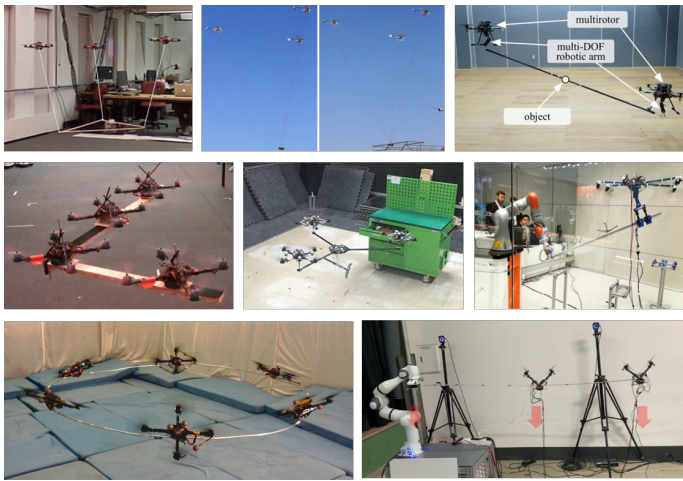
Fig. 4: Examples of aerial cooperative manipulation systems (from top, from left): 1) multi-quadrotor cable-suspended transport [7]; 2) multi-helicopter cable-suspended transport [12]; 3) cooperative aerial manipulators [128]; 4) rigidly-attached quadrotors [129]; 5) SmQ platform [130]; 6) MAGMaS platform [101]; 7) flexible ring cooperative manipulation [131]; and 8) distributed vibration suppression with RVMs [132].

in SE(3), compute the position of each quadrotor, which optimizes certain measures (e.g., Hessian of the payload pose) while satisfying certain feasibility conditions (e.g., positive cable tension, collision avoidance). However, the results of [7], [8] suffer from the multiple solutions of the forward kinematics, that is, given the quadrotors' position, the payload can subsume three-DoFs motion relative to the quadrotors. This issue was then resolved in [9] by enforcing so called "cone-constraint" of each quadrotor's position relative to the payload pose and other quadrotors' positions.

All the works in [7]–[9], [108] are yet kinematic results, thus, not able to realize high-speed dynamic payload transport with the quadrotor-payload dynamic coupling. This limitation was then addressed in [133] by formulating the quadrotor-payload system as a differentially-flat hybrid system (with the system of positive tension defining a differentially-flat sub-system and switching to other sub-system with the cable slack) and planning a dynamically-feasible trajectory for that. This dynamic cable-suspended transportation was also demonstrated using three small-size helicopters in [12], [13], where a two-DoFs cable angle sensor and a cable-tension sensor were installed to measure and compensate for the cable tension on the helicopter dynamics, an approach more suitable for large-size aerial robots with enough load-carrying capacity (see Figure 4). Two-quadrotor distributed cable-suspended manipulation of a rod payload with only onboard sensors (*i.e.*, monocular camera and IMU) was demonstrated in [134] with some simplifying assumptions (*i.e.*, two decoupled slung-load systems, no cable slack, straight trajectory, etc.) and also in [72], [73], [135] based on the leader-follower setting with the use of an admittance control together with a wrench observer.

Aiming for more precise pose control of the payload, the idea of deploying multiple aerial manipulators (*i.e.*, quadrotor with a multi-DoFs arm - see Section III) has been explored [128], [136]–[139]. One of the key challenges for this is

the complicated and high-dimensional dynamics of the total system, which is further exacerbated by the interaction with the environments/objects (e.g., unilateral grasping). The work of [136] solved this dynamics and presented a hierarchical control law when the multiple aerial manipulators grasp and manipulate a common rigid object via friction-cone contact constraint. Whereas, the work of [137] circumvented this dynamics complexity by utilizing two impedance control-loops (*i.e.*, object-level control and internal force regulation) with the rigid object grip assumption. Both of these works [136], [137] were validated only with simulations though.

The works of [128], [138], [139] presented frameworks for the cooperative manipulation of a rod-like object by using two aerial manipulators and their experimental demonstrations (see Figure 4). In [138], an adaptive sliding-mode control was presented to estimate and reject disturbances including the object's dynamics with the rigid-grip and equal object weight distribution assumptions. A RRT⋆-based path planning method was also devised to drive the object. The results of [138] were extended in [139] to incorporate obstacle avoidance, and the technique of RRT⋆-PDMPs was proposed, where the RRT⋆ was used for learning the motion parameters given the obstacle information in the form of DMP (dynamic movements primitives) for fast and robust path planning. A NSB (null-space based) control scheme was proposed in [128], where an inner-loop control was designed to robustly control each hexarotor while estimating and rejecting disturbances including their own arm dynamics, whereas the outer-loop control computed reference velocity for the system while incorporating internal force regulation and collision avoidance in an NSB hierarchy.

Another line of research for cooperative manipulation is to directly or rigidly attach multiple quadrotors on an object and use them as distributed actuators to transport and manipulate that object, thereby, overcoming the limitations of a single aerial robot while retaining mechanical simplicity. This idea was first demonstrated in [129], where four quadrotors were rigidly attached on a planar rigid payload of various shapes (e.g., L-shape, T-shape) with their thrust directions all normal to the payload surface. A two-norm optimal control was also derived and partially decentralized in [129] for scalability along with a special micro-spine mechanism to quickly grip the payload. The result of [129] was extended in [140], where two quadrotors were used to transport a rigid rod only with onboard sensing (*i.e.*, monocular camera and IMU) based on a nonlinear controller capable of more agile maneuvers.

The results of [129], [140] are more for transportation than for manipulation, as it is not possible to control the position and orientation of the object independently due to the well-known under-actuation property of the multi-rotors (with all the rotors parallel with each other). To overcome this issue of under-actuation, the SmQ (Spherically-connected Multi-Quadrotor) system was proposed in [130], [141], where multiple quadrotors were attached to a platform via spherical joints to render the platform fully-actuated (e.g., can maintain attitude during side-way motion) - see Figure 4. A dynamics-based control law, which also addressed the rotating limit of the spherical joints via constrained optimization, was designed and validated with various experimental demonstrations for the

SmQ platform in [130]. This spherical joint connection, which allows for omni-direciontal thrust generation, was adopted in [135] as well. Similarly in [142] (see Section VI).

In addition to purely aerial cooperative manipulation systems as discussed so far, there are recently emerging results on the mixed deployment of aerial and ground robots to exploit their complementary capabilities, that are: the ground robots often possess high load carrying ability, yet, with limited workspace, wheres the aerial robots possess unlimited workspace (and ability to easily increase moment-arm length), yet, with limited payload. The work of [143] presented a cooperative manipulation system consisting of a ground mobile robot and a quadrotor, where the position of a rigid object was controlled by the mobile robot while its tilting angle by the (spherically connected) quadrotor. However, the result of [143] is limited only for the sagittal plane similar to the case of a 2-DoFs pendulum-cart system. On the other hand, the MAGMaS (multiple aerial ground manipulator system) was proposed in [144], where a 7-DoFs KUKA LBR iiwa industrial manipulator and a (spherically connected) quadrotor were controlled to cooperatively manipulate a long rigid object, which was too heavy and too long to be individually handled by either robots (see Figure 4). This MAGMaS system was then extended in [101] with the spherical joint replaced by the OTHEX system [100] for higher and wider-angle thrust capacity with the bilateral teleoperation ability also added; and further expanded in [145], where the flexibility of the object, likely arising for long-slender or large-size/thin objects, was incorporated. The authors designed a control law for the cooperative manipulation of the flexible object while suppressing its vibration, proving its controllablity as well.

The area of aerial cooperative manipulation of flexible or soft objects has not been investigated much so far. The work of [131] considered the problem of cooperative handling a flexible ring by six quadrotors, each rigidly attached to the ring with some tilted angle to directly provide horizontal-direction control force (see Figure 4). The dynamics model of the ring with each quadrotor as wrench generator was linearized about the hovering configuration and Kalman estimation and LQR (linear quadratic regulator) were applied to regulate the ring pose while suppressing its vibration modes. Vibration control of a long flexible beam of skewed rectangular cross-section with distributed rotor-based vibration suppression modules (RVMs) was investigated recently in [132], where the two-rotor modules, whose design was optimized to maximize thrust force generation in the longitudinal-vertical plane with minimal torsional torque, were distributed along the beam. Further, optimal placement problem was solved by maximizing controllability Gramian and the vibration suppression was experimentally demonstrated (see Figure 4).

V. INTERCONNECTED ACTUATED MULTI-BODY DESIGNS

This section surveys a recently emerging class of aerial robotic platforms, which consist of multiple articulated links or bodies, that are mechanically connected with each other via passive or actuated joints and fly with tilted or tilting rotors distributed over them. This kind of platforms can fly while

Fig. 5: Examples of interconnected actuated multi-body designs (from top, from left): 1) HYDRUS [105]; 2) flying-gripper [146]; 3) distributed flight array (DFA) [147]; 4) DRAGON [148]; 5) flying LASDRA [149]; and 6) operation LASDRA [109].

changing their shape, thereby, can realize novel scenarios as: 1) aerial grasping of objects by directly using their bodies; 2) aerial operation in cluttered environment via serpentine motion; 3) very large-size robots, that can do aerial manipulation free from classical issues as short operation time, low payload, difficulty in control and sensing; and even 4) articulated flying characters in amusement parks.

The works of [105], [150], [151] presented the HYDRUS (transformable multi-rotor with two-dimensional multilinks) platform. Each link module consists of one rotor with enclosing cage and one servo-motor with its rotation axis parallel to the one of the rotor. Thereby, the robot can change its shape in the horizontal plane while retaining the hovering efficiency of typical multi-rotors. The platform also demonstrated whole-body aerial gripping and transport of a box-like object considering friction cone constraints, and the rotor and servo-motor actuation limitations (see Figure 5). This HYDRUS platform was also used in [152] to transport multiple objects at the same time by hanging them via cables. For this problem, the platform configuration, namelly the shape in the horizontal plane, is optimized to minimize the required thrust of each rotor while balancing the loading among the rotors. This HYDRUS was further extended in [104], where the HALO (Horizontal plane transformable Aerial robot with closed-LOop multilinks structure) platform was presented. HALO is based on HYDRUS, yet, making a closed-loop link to increase the platform rigidity while also using 20°-tilted rotors to improve the horizontal motion performance. HALO was used to transport a planar payload attached parallel to the platform through short cables to mitigate uncontrollable payload oscillations [9]. Again the platform configuration is optimized to minimize the mass-center offset between the platform and the payload reducing steady-state hovering torque. An evolution of such a vehicle that is fully-actuated has been

presented in [117].

Similar to HYDRUS and HALO platforms, one can find the flying gripper system proposed in [146]. It is designed as a modular closed-chain system, each module consisting of an off-the-shelf Crazyflie 2.0 quadrotor with a carbon fiber cuboid cage around it. An axially magnetized cylindrical Neodymium Iron Boron (NdFeB) magnet was attached on the vertical hinge of each cuboid to allow them to rotate about the thrust direction of the quadrotors. A four-cuboid flying gripper system was then constructed and experimented to grasp a paper cup by squeezing the aperture angle of the four-bar linkage closed-chain among the four cuboids (see Figure 5). Related to the previous platforms there is also the distributed flight array (DFA) of [147] (see Figure 5). It is also constructed as a modular system, each module consisting of a rotor and driving wheels, so that, only when they form an array (using the wheels), they can fly together. However, in this case the array structure is fixed and not actuated.

On the other hand, [148] proposes the DRAGON (Dual-rotor embedded multilink Robot with the Ability of multi-degree-of-freedom aerial transformatiON) platform, consisting of multiple carbon fiber pipe modules, on each of which two parallel rotors were attached via a two-DoFs thrust vectoring mechanism (*i.e.*, dual-rotor gimbal module). The pipe module itself was then connected with other modules via a two-DoFs orthogonal-axes joint with a pulley transmission with high reduction ratio. This reduces the back-drivability of the joint, thereby, mitigating possible vibration propagation through these joints. In contrast to the HYDRUS and HALO platforms, the DRAGON platform is fully-actuated, capable of assuming any pose and shape in SE(3) (up to the joint and rotor limits). Flying with fixed and changing shapes was experimentally demonstrated in [148] (see Figure 5), also performing pulling/pushing operations [106].

Another research along the same line is based on the LASDRA (Large-size Aerial Skeleton with Distributed Rotor Actuation) platform [109], [149]. Each link is based on the ODAR robot [81] and connected via string to maximize the dexterity of the motion. The LASDRA system aims at overcoming the well-known challenges in aerial manipulation (e.g., limited battery and payload, difficulty of onboard sensing and control, etc.) by making the robot large enough so that it can perform aerial manipulation tasks while tethered to the ground (or other vehicles). The "base" could provide abundant power and, consequently, the possibility of using powerful rotors. The mechanical structure of the LASDRA platform also provides the inherent stabilizing inertial/dissipative effects, while making the state estimation problem easier by enforcing the kinematic relations (measurable by, e.g., IMUs) from the (known) base to the end-effector.

Outdoor autonomous flights of a 3m-long 3-link 15-DoFs untethered LASDRA system was demonstrated in [149], where the estimation accuracy was substantially improved (*i.e.*, inter-link position RMSE less than 5cm) by fusing the kinematic constraints and the distributed IMU and GNSS sensors in the form of semi-distributed EKF (extended Kalman filtering). The method provides stable autonomous flight while avoiding excessive internal forces within the system (see Figure 5).

TABLE IV: Teleoperation features for aerial physical interaction.

Aerial platform		Reference	Human interface	Task	Level of maturity
Single	UDT	[154]	haptic	point contact and push	simulation
	MDT	[155]	haptic and 3D view	pick & place	experiment
Multiple	UDT	[142], [156]	haptic	manip.	simulation
	MDT	[101]	haptic	manip.	experiment

Various manipulation tasks with a 3m-long 2-link 6-DoFs operational LASDRA system were also demonstrated in [109], where compliant turning of an industrial valve was achieved based on the back-drivability of the BLDC rotors (see Figure 5). This LASDRA system is scalable, that is, with each link addressing its own weight, arbitrary number of links can be added indefinitely. To support this scalability, a distributed impedance control law was designed and applied to each individual link of the LASDRA systems [109], [149].

VI. TELEOPERATION

Because of the increasing number and complexity of applications in which aerial robots could be applied, methods that allow human intervention and supervision are required. It is indeed of fundamental importance, for safety and regulatory reasons, to let a human operator remain in the loop while the robotic system acts on the environment in an autonomous or semi-autonomous way [28]. The majority of the presented works on aerial teleoperation at date focused on the contact-free motion control of the vehicles (see, e.g., [126], [153] and references therein). Bilateral (e.g., with haptic feedback) teleoperation methods have been presented to help humans controlling single [153] and multiple aerial vehicles navigating in cluttered environments. In the following, we present the most important recent works on the teleoperation of aerial systems with particular regard to aerial physical interaction and manipulation. Table IV gathers the main features of the state of the art on teleoperation for aerial physical interaction.

Considering *uni-directional thrust platforms*, teleoperation solutions focused on the case in which the platform is equipped with a simple rigid tool. In [154] a bilateral haptic feedback method has been proposed to address tasks like point contact, and pull/push. To increase the payload and the manipulation capabilities, a similar solution for a multi-robot scenario is proposed in [142], [156]. In these works, the fleet of robots is employed as a flying hand to remotely manipulate objects. However, likely due to its complexity, such solution has been validated only in simulation.

To develop hardware-in-the-loop simulators for physical interaction tasks, the work in [157] uses an industrial arm equipped with an additional smaller manipulator to simulate an aerial manipulator interacting with the environment. The problem of rendering the robot dynamics and the interaction forces is addressed. The latter can be then used in a haptic-feedback scenario to test specific teleoperation methods.

Considering *multi-directional thrust and fully-actuated plat-forms*, the literature focused on designing teleoperation solu-

tions for pick & place tasks. The teleoperation of the cable-suspended aerial manipulator *SAM* equipped with an articulated arm is shown in [155]. The authors proposed the use of a 3D visual plus haptic feedback helping the user to drive the end-effector toward the grasp of a object. In [101], the authors addressed the teleoperation problem of a heterogeneous multi-robot system composed of aerial and ground manipulators that cooperatively manipulate long objects.

From the human point of view, the common feedback used to help the telemanipulation are:

- *Visual*: from robot to human, cameras mounted on the aerial platform or on the end-effector are employed to provide 2D or even 3D images [155] to the operator. These information can also be integrated with head mounted displays in a Virtual Reality (VR) framework [158], [159] helping the operator performing the task. On the other hand, in [156] a RGBD camera is used to extract human commands from the motion of his/her hand, which are then translated into robotic actions.
- *Haptic*: haptic devices provides a sense of touch to the human. Using delta type haptic devices, one can apply 3D forces to the human to augment his/her situation awareness. In [101], the haptic device is used to send the desired pose of the manipulated object from the human to the robotic system. In the other sense, it is used to apply on the human hand forces that are related to the inertia of the system and the presence of obstacles. In [154], the delta device is used to control the interaction forces of a quadrotor platform equipped with a rigid tool. The operator, moving the end-effector of the device, sends desired forces at the end-effector of the robot. On the other hand, the haptic device is used to apply to the user forces that give the perception of the contact force applied by the robot to the environment. These forces are also used to give the feeling of the distance from zero-commanded force.

VII. PERCEPTION AND PLANNING

A. Motivation and Requirements

Three phases can be distinguished in aerial manipulation operations: 1) navigation from the take-off position to the proximity of the workspace ensuring collision avoidance and reactivity in case of unexpected obstacles; 2) approaching to the desired operation position with higher accuracy; 3) manipulation with accurate position and interaction control.

Phases 1) and 2) should consider perception to avoid collisions of a load being transported, also involving perception-based localization and accurate SLAM in GNSS denied environments. Object detection, tracking and localization are required for grasping and manipulation in phase 3), being distinctive of aerial manipulators when compared to other aerial robots. Motion planning also requires particular care in aerial manipulation. The dynamic coupling between the manipulator and the aerial platform should be considered at the motion planning level to prevent undesired position deviations that may result in collisions with the environment. Therefore, the planner should consider the full body dynamics and compute an optimal trajectory for every DoF.

B. Perception

Perception functionalities are needed for localization and mapping as well as for object detection and manipulation.

1) Localization and mapping: UAV navigation is usually based on GNSS. The position provided by GNSS is used to close position control loops and to track desired trajectories. However, in many cases, the relative low frequency and the accuracy degradation due to the satellite visibility and communication problems, precludes its fully autonomous application. There are also many AEROM's applications in GNSS denied environments that require alternative approaches based on environment perception. In the following, we review localization methods and technologies for contact-free and manipulation operations, e.g., while transporting a load with the arms, or while performing contact-based inspection.

Odometry based on the combination of IMU and vision, with no absolute localization [160], is a well known approach that has been applied in aerial manipulation. In [39] visual-inertial fusion with event cameras is presented. The use of event cameras offers significant advantages over standard cameras providing a very high dynamic range, very small latency, and no motion blur which are relevant characteristics for AEROMs in non-controlled outdoor environments.

Visual localization and SLAM methods were also applied. Absolute 3D localization in the world frame $\mathcal{W}$ (see Figure 6) and mapping can be performed from measurements obtained by multi-modal sensorial approaches using 3D LIDAR, stereo cameras and radio range measurements w.r.t. beacons (see Chapter IV.2 of [43]). Ultra Wide Band (UWB) time-of-flight sensors are applied to compute the position of a receiver on-board the aerial robot, by means of triangulation and Range Only estimation, based on a decentralized Extended Information filter combined with a Particle Filter for initialization. This can be applied at relatively long distances but the emitters should be well distributed; the method is affected by reflections, and the orientation cannot be obtained. Moreover, they provide position estimation with only about $0.5\,\mathrm{m}$ accuracy. When the robot is tens of meters from objects, a 3D LIDAR provides a better accuracy and reliability. Finally, at small distances, stereo cameras can be applied and fuse the point clouds resulting from the camera with those provided by the 3D LIDAR. In [38] a Multi-Sensor 6-DoFs Localization method is applied. An Iterative Closest Point (ICP) algorithm extended to consider 3D-3D matchings between LIDAR (3D distances) or cameras (distances in the SURF space) is used in the prediction stage. Also, the ICP can be easily combined with the IMU, optimizing the joint (laser and camera) error. The method can be implemented in real time with moderate computational cost on-board the robot. These methods have been implemented without any marker and by using measurements obtained at tens of meters with RMS errors between $0.11\,\mathrm{m}$ and $0.21\,\mathrm{m}$. Greater accuracy in relative localization can be obtained by means of markers. In particular, with visual markers it is possible to obtain the position with an accuracy better than $5\,\mathrm{mm}$ at a distance of $0.7\,\mathrm{m}$ by means of image processing. The method, presented in Chapter IV.4 of [43], is based on optimizing the alignment of deformable contours

from textureless images.

2) Object detection: Object detection is strongly dependent on the used sensors. The payload of the aerial robot is a very important constraint. Then, visual cameras with light optics are the most used sensors. In aerial manipulation two different problems exist: the detection of objects to be manipulated at a certain distance (usually meters) in order to perform the approach, and the detection for grasping and manipulation. The first is a rough detection based on: 1) features, related for example to shape and color; 2) templates of the target object, which could be fixed or deformable to adapt to changes of the viewing angle due to the motion of the aerial robot; and 3) classifiers, which could be also based on particular features. Moreover, there are methods based on motion analysis that also use features or templates. The deep learning classifiers extracting image features are being applied more and more.

On the other hand, the detectors for grasping and manipulation should provide high accuracy. Methods based on markers, *i.e.*, fiducial markers, have been proposed. In Chapter IV.6 of [43] markers detection libraries and deep learning are applied. It is also possible to avoid the use of markers and apply modeling techniques of the objects to be manipulated. Particularly, Gaussian Process Implicit Surfaces (GPIS) [161] takes into account the environment uncertainties involved in computer vision. This probabilistic information has been used in the H2020 AEROARMS project to generate grasp configurations. Moreover, the model is used to compute the relative 3D pose. Figure 6 shows an outdoor crawler detection and grasping with a dual arm. The GPIS models the crawler surface computing a covariance term for each point of the approximated surface. Alternatively, RGB-D cameras and Convolutional Neural Networks (CNN) can be used to obtain in real-time a suitable model for grasping. The state variables in the estimation of points of the object in the camera reference frame of Figure 6 is given by $[^C\boldsymbol{p}_{[t]}, {}^C\boldsymbol{\eta}_{[t]}, {}^C\dot{\boldsymbol{p}}_{[t]}, {}^C\boldsymbol{\omega}_{[t]}]^\top$, where $^C\boldsymbol{p}_{[t]}$, $^C\boldsymbol{\eta}_{[t]}$, $^C\dot{\boldsymbol{p}}_{[t]}$ and $^C\boldsymbol{\omega}_{[t]}$ are respectively the position, orientation, linear velocity and angular velocity in the camera frame $\mathcal{C}$ shown in Figure 6 at the time instant t. These variables can be estimated by means of an Extended Kalman Filter. The resulting estimations of the centroid of the object to be grasped $^C\boldsymbol{p}$, $^C\boldsymbol{\eta}$ are used to compute the grasping points of the bar handle by means of the model of the object. Then, the references for the grasping point of each arm can be obtained as $[^E\boldsymbol{p}^i, {}^E\boldsymbol{\eta}^i]^\top = {}^E\boldsymbol{T}_C^i[^C\boldsymbol{p}_{[t]}, {}^C\boldsymbol{\eta}_{[t]}]^\top$, where $^E\boldsymbol{p}^i$ and $^E\boldsymbol{\eta}^i$ for $i = 1, 2$ are the position and orientation of the grasping points for the arms in the End-Effector frame, $\mathcal{E}$, and $^E\boldsymbol{T}_C^i$ is the transformation from $\mathcal{C}$ to $\mathcal{E}$ for the arm i. These references can be passed to control methods described in Section III. Position based [27], [162] or image-based visual servoing [40], [163] can be used, expressing the error and control inputs directly in the image space, minimizing the error w.r.t. desired image feature coordinates.

C. Planning

1) Planning levels: The higher level in planning of aerial manipulators is mission planning, e.g., the plan to assemble a structure from separate parts by taking into account the
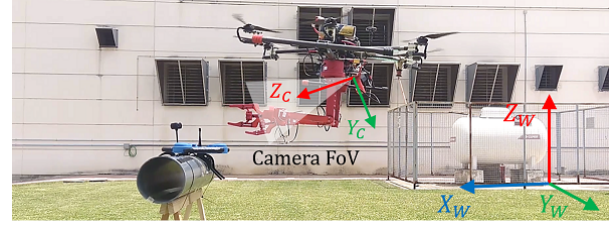

Fig. 6: Aerial manipulator grasping a crawler.

Fig. 7: Two aerial manipulators assembling a structure (left). Long reach aerial manipulator with dual arm transporting a bar (right).

constraints related to the final desired state, the location of the parts, the connectors and the tools (see Figure 7 left). The second level is the planning of the individual tasks to achieve the previously obtained assembly plan. In case there are several aerial robots, the task planner should allocate tasks to the different robots. The lower level is the motion planner, which is in charge of computing the trajectories of the robots, in such a way that the end-effectors of the aerial manipulators perform the previously specified tasks.

The above decomposition simplifies the inherent complexity of the aerial manipulation planning. Assembly and task planning are symbolic and consist of sequences of actions. These actions involve the motion of the aerial robots whose feasibility should be checked taking into account constraints, including the geometric ones. In [164] task and motion planning are interleaved in such a way that geometric constraints involved in the symbolic actions are checked and the plans are modified until the geometric constraints are satisfied. This requires to build and maintain a geometric counterpart of the symbolic plan to ensure that the current geometric state matches the current symbolic state.

2) Assembly and Task Planning levels: The Assembly Planning (AP) uses a 3D CAD model of the structure and generates the tuple $PR = \langle S, D \rangle$, where $S = \{s_1, ..., s_n\}$ is the ordered sequence of operations to assemble the structure and $D = \{d_1, ..., d_m\}$ is a set of dependencies between assembly operations. The dependency d_j is a tuple made of the target operation and the set of all other operations that should necessarily be performed before that one, with $d_j = \langle t_l, p_k \rangle$ which is the set of operations p_k that should be achieved before the operation t_l, where t_l is just the identifier of an operation s_l. The set p_k contains the list of identifiers for operations from S. The AP should take into account the connections between parts and the involved forces. Considering truss structure built with connectors and links (see Figure 7 on the left), interaction and gravity forces should be considered for their assembly. There are tools, such as the Bullet Physics library, that can be

used to check if a subset of assembled parts is self-sustaining and can remain indefinitely to the given configuration without external support (statically stable).

AP is an NP-hard problem [165], which can be represented using directed graphs where each vertex and edge represents an assembly component and the corresponding relationship, respectively. Each candidate sequence can be evaluated by an objective cost function to be optimized or by a penalty value if the candidate sequence leads to an unstable configuration. In [165], a discrete particle swarm optimization algorithm is applied. In [166] reverse disassembly sequences are used to determine the assembly, providing faster eliminations thanks to the increased number of constraints at the beginning. The assembly plan can be implemented using several aerial robots. Thus, the planner tries to combine successive actions into parallel operations to be executed at the same time by separate robots. The work in Chapter V.1 of [43] implements interleaved task and motion planning of aerial robots by means of a Geometric Task Planner to perform the assembly of a truss structure. It includes actions devoted to the monitoring of the assembly actions by means of visual tracking of the robots. The resulting symbolic task plan has associated motions that should be also planned as follows.

3) Motion Planning: Many practical approaches for motion planning of aerial manipulators decouples the problem of the planning of the aerial platform and the manipulator. First, the algorithm plans a trajectory of the Center of Gravity (CoG) of the aerial platform that ends in a suitable position for manipulation, then the algorithm plans the motion of the end-effector, assuming that the aerial platform maintains the same position and orientation during the manipulation. These approaches have the following drawbacks: 1) The geometric approach is not able to deal with the orientation, which plays an important role in aerial manipulation; 2) The decoupling between the aerial platform and the manipulator could be inefficient from the energy point of view and execution time; 3) The above decoupling could be unfeasible when the motion of the robotic manipulator is needed to avoid obstacles (see Figure 7); and 4) The decoupling is also unfeasible when the motion of the manipulator has significant impact on the motion of the platform.

Kinodynamic planning allows the consideration of the kinematic and dynamic constraints in the motion of the aerial manipulator. A simple decoupling approach consists of a first step of geometric planning for a sphere bounding the aerial platform, by using, for example, RRT to compute segments with zero velocity and acceleration at end-points. Then the path is transformed in a trajectory satisfying the kinematic and dynamic constraints. Finally, velocity and accelerations are modified along the local paths without modifying its geometry and ensuring collision avoidance [167]. In [168] control aware planning is proposed to maintain contact with a surface. There are also methods that consider jointly motion planning and control to maintain this contact [94]. In the AEROARMS project an RRT* algorithm was used for planning the simultaneous motion of the aerial platform and the joints of the arms transporting a bar in an environment with high density of obstacles, as shown in Figure 7. A planar model with eight

configuration variables for the aerial manipulator was used. The motion of the arms of the long reach aerial manipulator in Figure 7 right when holding the bar, modifies the position of the CoG of the aerial robot and then the motion of the aerial platform. If this coupling is not considered, collisions may occur. In order to avoid these collisions an RRT* with dynamic awareness has been developed and implemented [169].

4) Reactivity: Aerial robots are often subject to disturbances, including non-modelled aerodynamic effects, positioning inaccuracy and others. This is particularly true for small outdoor aerial robots where the wind plays a significant role. Moreover, it is also difficult to consider all the unexpected objects and forces that could be involved in aerial manipulation. Then, reactivity is needed to increase the safety of AEROMs. Autonomous reactivity should be based on the perception capabilities of the AEROM, by including mainly range sensors, computer vision and force/torque sensors. The above mentioned perception, planning and reactivity functionalities were integrated for real-time execution in the AEROARMS project [28]. The system was implemented with an on-board 3D laser and a computer to perform mapping and motion planning in real time (see Figure 7 right).

VIII. New Generation of AEROMs

A. Challenges

1) Time of flight and range: The current time of flight of most AEROMs are minutes or tens of minutes, which is too short for many practical applications. The increasing of the flight time involves new configurations of aerial platforms, new sources of energy and even new control and motion planning methods. Some applications also require increased range, involving flights beyond the visual line of sight, which also implies the respect of regulations and safety norms.

2) Safety in the interactions with persons and objects: AEROMs are based on multi-rotors and helicopters. The energy of the propellers is a threat for people and valuable objects close the aerial manipulator. This is particularly true for applications such as aerial co-workers for physical interactions (see Figure 8). Thus, it is necessary to develop safer platforms and new technologies to enhance safety.

3) Accuracy: The accuracy of AEROMs depends on the accuracy of the positioning sensors, and is limited by unavoidable perturbations, such as wind gust and aerodynamic effects due to nearby surfaces. Some of these effects can be modeled and controlled, but others are difficult to manage, especially with the limited on-board capabilities of light AEROMs.

4) Reliable decisional autonomy: Current AEROMs usually require human supervision. The increasing of decisional autonomy should involve high reliability by considering all the sources of faults and contingency measures.

Crossed effects between challenges are also present, e.g., the increase of decisional autonomy requires high on-board computational capabilities that are constrained by the minimization of payload to increase flight time and range.

B. Approaches

1) Energy: There are different approaches to save energy and thus increase the time of flight or the range.

• Perching. Most research works in aerial manipulation assume that the operation is carried out in flight. However, in some cases, the robot could perch on support structures like poles or cables to avoid the waste of energy and extend the operation time. Some mechanisms for quadrotor perching have been proposed, including bioinspired passive mechanisms [170], grippers [171] or vacuum cups [172].

• Hybrid aerial-ground platforms. Aerial locomotion requires significantly more energy than ground locomotion. Vehicles with hybrid locomotion can fly to sites that cannot be accessed by ground, land, perform the final approach by means of ground locomotion, and finally perform the task from the ground or attached to a static surface. This saves energy and increases the operation time [173].

• Hybrid fixed/rotary-wing platforms. This includes aerial platforms integrating the beneficial features of fixed-wing (long flight time and range) and rotary-wing (vertical take-off and landing and hovering). In [174], these platforms are categorized into two types: convertiplanes and tail sitters. The former maintains the airframe orientation and switch between flight modes. It includes the tilt-wing platform [175] where the wing is partially or totally tilted together with the rotors during the flight-mode transition, and also dual-systems which have two sets of propulsion units: upward and forward mounted rotors for vertical motion and cruise flight, respectively. On the other hand, the tail sitter performs take-off and landing vertically on its tail while the entire airframe tilts to achieve cruise flight [176]. None of these platforms have been used up to now for aerial manipulation.

• Morphing and bioinspired approaches. These include configurations inspired by birds and insects. Particularly, morphing technologies can be applied to change between a low drag configuration, typical in fixed wings, and high lift configuration to avoid stall at low speeds or even to hover [177]. It has also been shown that flapping-wing flight, so abundant in nature, is more efficient than rotary-wing flight [178], [179]. It is well known that birds are able to fly long distances minimizing the energy consumption. Several flapping unmanned aerial vehicles, called ornithopters, have been designed. The key aspect to save energy is the optimal combination of gliding and flapping. It has been also shown that the drag of the flapping wing is greater than fixed wing. Thus, the flap-gliding flight yields a performance advantage when comparing with only flapping. Furthermore, the maximum range performance achievable with flap-gliding flight and the associated optimal travelling speed have been determined [180]. In order to perform the optimal switching between flapping and fixed wing phases, it is necessary to obtain the velocity and height from which to start descending at a very low angle, maximizing the lift to drag ratio. Also the transitions from gliding to flapping to increase altitude or to perform perching is very important. Suitable models and new control and planning methods should be obtained. However, up to now, flapping-wing platforms have not been used for aerial manipulation. The ERC Advanced Grant GRIFFIN proposes the development of new bio-inspired aerial manipulation systems with the capability to glide, saving energy, flap the wings, perch, fold the wing and manipulate. Reference [53]

Fig. 8: AEROM providing a tool (left) and guiding a human (right).

introduced the concept of winged aerial manipulation robot, combining the manipulation with gliding to reduce the total weight of the aerial robot.

2) Safety: It involves both information processing and physical interactions. The former is related to situational awareness including environment perception for collision detection and avoidance. The second is related to AEROMs physically interacting with humans [181] (see Figure 8), e.g., to provide tools at height [34] or to help in manipulation tasks.

3) Accuracy: The modeling and control of the aerodynamic effects can be considered to increase the accuracy of aerial manipulators in free flight. The sensing of airflow [182], the increasing of the control frequency, and implementations with new light servomotors, can be also used to cancel perturbations and increase the accuracy. Since the cancellation of all perturbations is difficult, an alternative strategy consists in manipulating the environment while perching or holding a fixed support with another arm.

4) Decisional autonomy and Reliability: The complexity of the implementation of autonomous functionalities is related to the conditioning of the environment. The use of markers facilitates autonomous perception as mentioned in Section VII-B. However, the variability of lighting conditions, as it is usually the case outdoors, plays an important role. On the other hand, perturbations are unavoidable and the aerial manipulator will deviate from the planned trajectory due, e.g., to wind gusts or to uncontrolled aerodynamic effects. It is then necessary to apply methods from Section VII-C to provide reactivity based on the perception of the environment. It is quite possible that, during manipulation operation, external perturbations will generate collisions. The effect of these collisions can be greatly reduced by having compliance, as shown in Section III. However, compliance worsens the accuracy. Thus, adaptive compliance should be a characteristic of future aerial manipulators.

The decisional autonomy is related to the on-board sensing, actuation and computational capabilities. However, the hardware to implement these capabilities is constrained by the weight and energy consumption. Future processors will favor the implementation.

IX. CONCLUSION

In this manuscript, we revised aerial robotic manipulation. This is a constantly growing domain in which we analyzed every aspect characterizing autonomous robots, ranging from the design and control of aerial manipulators to the perception and motion planning problems for physical interaction tasks.

Our analysis evinces that the research on aerial manipulation already provided aerial robots with great physical interaction capabilities. However, most of the experimental works done so far have been conducted in structured indoor environments. Nevertheless, with the aim of increasing the precision and robustness of aerial manipulators for their application in real environments, the number of outdoor experimental investigations is increasing. These studies address all the challenges related to disturbances and uncertainty in outdoor conditions (e.g., wind gust, illumination, etc.) that dramatically impact robot performance.

Still, the great potential impact of aerial manipulation already pushed its use for industrial applications. Contact-based inspection is one of the first applications addressed but others will follow in domains like construction and maintenance. The challenges for the future and new approaches are related to the energy, safety, accuracy and reliable decisional autonomy.

REFERENCES

[1] A. Albers, S. Trautmann, T. Howard, Trong Anh Nguyen, M. Frietsch, and C. Sauter. Semi-autonomous flying robot for physical interaction with environment. In *2010 IEEE Conference on Robotics, Automation and Mechatronics*, pages 441–446, June 2010.

[2] D. Mellinger, Q. Lindsey, M. Shomin, and V. Kumar. Design, modeling, estimation and control for aerial grasping and manipulation. In *2011 Proc. of the IEEE/RSJ Int. Conf. on Intelligent Robots and Systems (IROS)*, pages 2668–2673, San Francisco, CA, Sep. 2011.

[3] Q. Lindsey, D. Mellinger, and V. Kumar. Construction with quadrotor teams. *Autonomous Robots*, 33, 10 2012.

[4] L. Marconi, R. Naldi, and L. Gentili. Modelling and control of a flying robot interacting with the environment. *Automatica*, 47(12):2571 – 2583, 2011.

[5] T. Danko C. Korpela and P. Oh. Mm-uav: Mobile manipulating unmanned aerial vehicle. *Journal of Intelligent & Robotic Systems*, 65(1-4):93–101, 2012.

[6] M. Fumagalli, R. Naldi, A. Macchelli, F. Forte, Arvid Keemink, S. Stramigioli, R. Carloni, and L. Marconi. Developing an aerial manipulator prototype: Physical interaction with the environment. *Robotics I& Automation Magazine, IEEE*, 21:41–50, 9 2014.

[7] N. Michael, J. Fink, and V. Kumar. Cooperative manipulation and transportation with aerial robots. In *Robotics: Science and Systems*, 2009.

[8] N. Michael, J. Fink, and V. Kumar. Cooperative manipulation and transportation with aerial robots. *Autonomous Robots*, 30(1):73–86, 2011.

[9] J. Fink, N. Michael, S. Kim, and V. Kumar. Planning and control for cooperative manipulation and transportation with aerial robots. *International Journal of Robotics Research*, 30(3):324–334, 2011.

[10] Q. Jiang and V. Kumar. The inverse kinematics of cooperative transport with multiple aerial robots. *IEEE Transactions on Robotics*, 29(1):136–145, 2013.

[11] P. E. I. Pounds, D. R. Bersak, and A. M. Dollar. Stability of small-scale uav helicopters and quadrotors with added payload mass under pid control. *Autonomous Robots*, 33(1-2):129–142, 2012.

[12] M. Bernard, K. Kondak, and G. Hommel. Load transportation system based on autonomous small size helicopters. *The Aeronautical Journal*, 114(1153):191–198, 2010.

[13] M. Bernard, K. Kondak, I. Maza, and A. Ollero. Autonomous transportation and deployment with aerial robots for search and rescue missions. *Journal of Field Robotics*, 28(6):914–931, 2011.

[14] P. E. Pounds and Aaron Dollar. Hovering stability of helicopters with elastic constraints. In *Dynamic Systems and Control Conference*, volume 44182, pages 781–788, 2010.

[15] P. E. I. Pounds and A. M. Dollar. Stability of helicopters in compliant contact under pd-pid control. *IEEE Transactions on Robotics*, 30(6):1472–1486, 2014.

[16] P. Pounds, D. Bersak, and A. Dollar. Grasping from the air: Hovering capture and load stability. In *2011 IEEE International Conference on Robotics and Automation*, pages 2491 – 2498, 06 2011.

[17] P. E. Pounds and Aaron M Dollar. Aerial grasping from a helicopter uav platform. In *Experimental Robotics*, pages 269–283. Springer, 2014.

[18] K. Kondak, F. Huber, M. Schwarzbach, M. Laiacker, D. Sommer, M. Bejar, and A. Ollero. Aerial manipulation robot composed of an autonomous helicopter and a 7 degrees of freedom industrial manipulator. In *2014 IEEE international conference on robotics and automation (ICRA)*, pages 2107–2112. IEEE, 2014.

[19] F. Huber, Konstantin K., K. Krieger, D. Sommer, M. Schwarzbach, M. Laiacker, I. Kossyk, S. Parusel, S. Haddadin, and A. Albu-Schäeffer. First analysis and experiments in aerial manipulation using fully actuated redundant robot arm. *IEEE/RSJ International Conference on Intelligent Robots and Systems*, 11 2013.

[20] A. E. Jimenez-Cano, J. Martin, G. Heredia, A. Ollero, and R. Cano. Control of an aerial robot with multi-link arm for assembly tasks. In *2013 IEEE International Conference on Robotics and Automation*, pages 4916–4921, May 2013.

[21] M. Kamel, K. Alexis, and R. Siegwart. Design and modeling of dexterous aerial manipulator. In *2016 IEEE/RSJ International Conference on Intelligent Robots and Systems (IROS)*, pages 4870–4876, Oct 2016.

[22] T. W. Danko, K. P. Chaney, and P. Y. Oh. A parallel manipulator for mobile manipulating uavs. In *IEEE Intl. Conference on Technologies for Practical Robot Applications*, pages 1–6, 2015.

[23] T. W. Danko and P. Y. Oh. A hyper-redundant manipulator for mobile manipulating unmanned aerial vehicles. In *International Conference on Unmanned Aircraft Systems (ICUAS)*, pages 974–981, 2013.

[24] M. Kobilarov. Nonlinear trajectory control of multi-body aerial manipulators. *Journal of Intelligent I& Robotic Systems*, 73(1):679–692, 1 2014.

[25] K. Morton and L. F. G. Toro. Development of a robust framework for an outdoor mobile manipulation uav. In *2016 IEEE Aerospace Conference*, pages 1–8, March 2016.

[26] V. Lippiello, J. Cacace, A. Santamaria-Navarro, J. Andrade-Cetto, M. A. Trujillo, Y. R. Rodríguez Esteves, and A. Viguria. Hybrid visual servoing with hierarchical task composition for aerial manipulation. *IEEE Robotics and Automation Letters*, 1(1):259–266, Jan 2016.

[27] C. Kanellakis, M. Terreran, D. Kominiak, and G. Nikolakopoulos. On vision enabled aerial manipulation for multirotors. In *2017 22nd IEEE International Conference on Emerging Technologies and Factory Automation (ETFA)*, pages 1–7, Sep. 2017.

[28] A. Ollero, G. Heredia, A. Franchi, G. Antonelli, K. Kondak, A. Sanfeliu, A. Viguria, J. R. Martinez-de Dios, F. Pierri, J. Cortes, A. Santamaria-Navarro, M. A. Trujillo Soto, R. Balachandran, J. Andrade-Cetto, and A. Rodriguez. The aeroarms project: Aerial robots with advanced manipulation capabilities for inspection and maintenance. *IEEE Robotics Automation Magazine*, 25(4):12–23, 2018.

[29] D. Brescianini and R. D'Andrea. Computationally efficient trajectory generation for fully actuated multirotor vehicles. *IEEE Transactions on Robotics*, 34(3):555–571, 2018.

[30] M. Kamel, S. Verling, O. Elkhatib, C. Sprecher, P. Wulkop, Z. Taylor, R. Siegwart, and I. Gilitschenski. The voliro omniorientational hexacopter: An agile and maneuverable tiltable-rotor aerial vehicle. *IEEE Robotics & Automation Magazine*, 25(4):34–44, 2018.

[31] M. Tognon and A. Franchi. Omnidirectional aerial vehicles with unidirectional thrusters: Theory, optimal design, and control. *IEEE Robotics and Automation Letters*, 3(3):2277–2282, 2018.

[32] M. Ryll, . Muscio, F. Pierri, E. Cataldi, G.Antonelli, F. Caccavale, D. Bicego, and A. Franchi. 6d interaction control with aerial robots: The flying end-effector paradigm. *The International Journal of Robotics Research*, 38(9):1045–1062, 2019.

[33] M. Orsag, C. Korpela, P. Oh, and S. Bogdan. *Aerial manipulation*. Springer Verlag, 2018.

[34] A. Suarez, F. Real, V. M. Vega, G. Heredia, A. Rodriguez-Castaño, and A. Ollero. Compliant bimanual aerial manipulation: Standard and long reach configurations. *IEEE Access*, 8:88844–88865, 2020.

[35] H. Paul, R. Miyazaki, R. Ladig, and K. Shimonomura. Landing of a multirotor aerial vehicle on an uneven surface using multiple onboard manipulators. In *2019 IEEE/RSJ International Conference on Intelligent Robots and Systems (IROS)*, pages 1926–1933, 2019.

[36] A. Suarez, G. Heredia, and A. Ollero. Design of an anthropomorphic, compliant, and lightweight dual arm for aerial manipulation. *IEEE Access*, 6:29173–29189, 2018.

[37] A. Pumarola , A. Vakhitov, A. Agudo, F. Moreno-Noguer, and A. Sanfeliu. Relative localization for aerial manipulation with pl-slam. In *Aerial Robotic Manipulation*, pages 239–248. Springer Tracts in Advanced Robotics, 2019.

[38] J. Paneque, J. R. Martinez-de Dios, and A. Ollero. Multi-sensor 6-dof localization for aerial robots in complex gnss-denied environments. In *2020 IEEE/RSJ International Conference on Intelligent Robots and Systems*, pages 1978–1984, 11 2019.

[39] E. Mueggler, G. Gallego, H. Rebecq, and D. Scaramuzza. Continuous-time visual-inertial odometry for event cameras. *IEEE Transactions on Robotics*, 34(6):1425–1440, Dec 2018.

[40] A. Santamaria-Navarro, P. Grosch, V. Lippiello, J. Solà, and J. Andrade-Cetto. Uncalibrated visual servo for unmanned aerial manipulation. *IEEE/ASME Transactions on Mechatronics*, 22(4):1610–1621, 2017.

[41] A. Caballero, M. Bejar, and A. Ollero. On the use of velocity adaptation to outperform the motion planning with dynamics awareness in aerial long-reach manipulators with two arms. In *2018 International Conference on Unmanned Aircraft Systems (ICUAS)*, pages 1125–1133, June 2018.

[42] A. Caballero, A. Suarez, F. Real, V. M. Vega, M. Bejar, A. Rodriguez-Castaño, and A. Ollero. First experimental results on motion planning for transportation in aerial long-reach manipulators with two arms. In *2018 IEEE/RSJ International Conference on Intelligent Robots and Systems (IROS)*, pages 8471–8477, 2018.

[43] A. Ollero and B. Siciliano, editors. *Aerial robotic manipulation*. STAR Springer tracts in advanced robotics, July 2019.

[44] M. A. Trujillo, J. R. Martinez-de Dios, C. Martin, A. Viguria, and A. Ollero. Novel aerial manipulator for accurate and robust industrial ndt contact inspection: a new tool for the oil and gas inspection industry. *Sensors*, 19:1305, 2019.

[45] Angel Flores-Abad, Ou Ma, Khanh Pham, and Steve Ulrich. A review of space robotics technologies for on-orbit servicing. *Progress in Aerospace Sciences*, 68:1–26, 2014.

[46] Ingrid Schjølberg and Thor I Fossen. Modelling and control of underwater vehicle-manipulator systems. In *in Proc. rd Conf. on Marine Craft maneuvering and control*. Citeseer, 1994.

[47] Junku Yuh. Design and control of autonomous underwater robots: A survey. *Autonomous Robots*, 8(1):7–24, 2000.

[48] A. Suarez, V. M. Vega, M. Fernandez, G. Heredia, and A. Ollero. Benchmarks for aerial manipulation. *IEEE Robotics and Automation Letters*, 5(2):2650–2657, 2020.

[49] A. E. Jimenez-Cano, P. J. Sanchez-Cuevas, P. Grau, A. Ollero, and G. Heredia. Contact-based bridge inspection multirotors: Design, modeling, and control considering the ceiling effect. *IEEE Robotics and Automation Letters*, 4(4):3561–3568, Oct 2019.

[50] Xiangdong Meng, Yuqing He, and Jianda Han. Survey on aerial manipulator: System, modeling, and control. *Robotica*, 38(7):1288–1317, 2020.

[51] F. Ruggiero, V. Lippiello, and A. Ollero. Aerial manipulation: A literature review. *IEEE Robotics and Automation Letters*, 3(3):1957–1964, July 2018.

[52] A. Martín-Alcántara, P. Grau, R. Fernandez-Feria, and A. Ollero. A simple model for gliding and low-amplitude flapping flight of a bio-inspired uav. In *2019 International Conference on Unmanned Aircraft Systems (ICUAS)*, pages 729–737, June 2019.

[53] A. Suarez , P. Grau, G. Heredia, and A. Ollero. Winged aerial manipulation robot with dual arm and tail. *Applied Sciences*, 10(14):4783, 2020.

[54] M. Hamandi, F. Usai, Q. Sablé, N. Staub, M. Tognon, and A. Franchi. Survey on Aerial Multirotor Design: a Taxonomy Based on Input Allocation. *Int. Journal of Robotics Research*, 2021.

[55] A. Franchi, R. Carli, D. Bicego, and M. Ryll. Full-pose tracking control for aerial robotic systems with laterally-bounded input force. *IEEE Transactions on Robotics*, 34(2):534–541, 2018.

[56] M. Ryll, H. H. Bülthoff, and P. Robuffo Giordano. A novel over-actuated quadrotor unmanned aerial vehicle: modeling, control, and experimental validation. *IEEE Trans. on Control Systems Technology*, 23(2):540–556, 2015.

[57] A. De Luca and G. Oriolo. Trajectory planning and control for planar robots with passive last joint. *Int. Journal of Robotics Research*, 21(5-6):575–590, 2002.

[58] H. Yang and D. J. Lee. Dynamics and control of quadrotor with robotic manipulator. In *2014 Proc. of the IEEE Int. Conf. on Robotics & Automation (ICRA)*, pages 5544–5549, Hong Kong, China, May. 2014.

[59] J. Welde, J. Paulos, and V. Kumar. Dynamically feasible task space planning for underactuated aerial manipulators. *IEEE Robotics and Automation Letters*, 6(2):3232–3239, 2021.

[60] H. Nguyen and D. Lee. Hybrid force/motion control and internal dynamics of quadrotors for tool operation. In *2013 Proc. of the IEEE/RSJ Int. Conf. on Intelligent Robots and Systems (IROS)*, pages 3458–3464, Tokyo, Japan, Nov. 2013.

[61] B. Yüksel, G. Buondonno, and A. Franchi. Differential flatness and control of protocentric aerial manipulators with any number of arms and mixed rigid-/elastic-joints. In *2016 Proc. of the IEEE/RSJ Int. Conf. on Intelligent Robots and Systems (IROS)*, pages 561–566, Daejeon, South Korea, Oct. 2016.

[62] D. Bicego, J. Mazzetto, M. Farina, R. Carli, and A. Franchi. Nonlinear model predictive control with actuator constraints for multi-rotor aerial vehicles. *Journal of Intelligent & Robotics Systems*, 3(100):1213–1247, 2020.

[63] M. Fumagalli, R. Naldi, A. Macchelli, R. Carloni, S. Stramigioli, and L. Marconi. Modeling and control of a flying robot for contact inspection. In *2012 IEEE/RSJ International Conference on Intelligent Robots and Systems*, pages 3532–3537, 2012.

[64] F. Forte, R. Naldi, A. Macchelli, and L. Marconi. Impedance control of an aerial manipulator. In *2012 American Control Conference (ACC)*, pages 3839–3844. IEEE, 2012.

[65] V. Lippiello and F. Ruggiero. Exploiting redundancy in cartesian impedance control of UAVs equipped with a robotic arm. In *2012 Proc. of the IEEE/RSJ Int. Conf. on Intelligent Robots and Systems (IROS)*, pages 3768–3773, Vilamoura, Portugal, Oct. 2012.

[66] M. Tognon, H. A. Tello Chávez, E. Gasparin, Q. Sablé, D. Bicego, A. Mallet, M. Lany, G. Santi, B. Revaz, J. Cortés, and A. Franchi. A truly redundant aerial manipulator system with application to push-and-slide inspection in industrial plants. *IEEE Robotics and Automation Letters*, 4(2):1846–1851, 2019.

[67] J. L. J. Scholten, M. Fumagalli, S. Stramigioli, and R. Carloni. Interaction control of an uav endowed with a manipulator. In *2013 IEEE International Conference on Robotics and Automation*, pages 4910–4915, 2013.

[68] V. Lippiello, G. A. Fontanelli, and F. Ruggiero. Image-based visual-impedance control of a dual-arm aerial manipulator. *IEEE Robotics and Automation Letters*, 3(3):1856–1863, 2018.

[69] A. Suarez, G. Heredia, and A. Ollero. Physical-virtual impedance control in ultralightweight and compliant dual-arm aerial manipulators. *IEEE Robotics and Automation Letters*, 3(3):2553–2560, July 2018.

[70] G. Antonelli, E. Cataldi, G. Muscio, M. Trujillo, Y. Rodriguez, F. Pierri, F. Caccavale, A. Viguria, S. Chiaverini, and A. Ollero. Impedance control of an aerial-manipulator: Preliminary results. In *2016 Proc. of the IEEE/RSJ Int. Conf. on Intelligent Robots and Systems (IROS)*, pages 3848–3853, Daejeon, South Korea, 2016.

[71] F. Ruggiero, J. Cacace, H. Sadeghian, and V. Lippiello. Impedance control of VToL UAVs with a momentum-based external generalized forces estimator. In *2014 Proc. of the IEEE Int. Conf. on Robotics & Automation (ICRA)*, pages 2093–2099, Hong Kong, China, Apr. 2014.

[72] M. Tognon, C. Gabellieri, L. Pallottino, and A. Franchi. Aerial co-manipulation with cables: The role of internal force for equilibria, stability, and passivity. *IEEE Robotics and Automation Letters, Special Issue on Aerial Manipulation*, 3(3):2577 – 2583, 2018.

[73] C. Gabellieri, M. Tognon, D. Sanalitro, L. Palottino, and A. Franchi. A study on force-based collaboration in swarms. *Swarm Intelligence*, 14:57–82, 2020.

[74] F. Augugliaro and R. D'Andrea. Admittance control for physical human-quadrocopter interaction. In *12th European Control Conference*, pages 1805–1810, Zurich, Switzerland, Jul. 2013.

[75] G. Heredia, A. E. Jimenez-Cano, I. Sanchez, D. Llorente, V. Vega, J. Braga, J. A. Acosta, and A. Ollero. Control of a multirotor outdoor aerial manipulator. In *2014 IEEE/RSJ International Conference on Intelligent Robots and Systems*, pages 3417–3422, 2014.

[76] B. Yüksel, C. Secchi, H. H. Bülthoff, and A. Franchi. Aerial physical interaction via IDA-PBC. *Int. Journal of Robotics Research*, 38(4):403421, 2019.

[77] R. Rashad, J. B. C. Engelen, and S. Stramigioli. Energy tank-based wrench/impedance control of a fully-actuated hexarotor: A geometric port-hamiltonian approach. In *2019 International Conference on Robotics and Automation (ICRA)*, pages 6418–6424, 2019.

[78] M. Tognon, S. S. Dash, and A. Franchi. Observer-based control of position and tension for an aerial robot tethered to a moving platform. *IEEE Robotics and Automation Letters*, 1(2):732–737, 2016.

[79] M. Tognon and A. Franchi. Dynamics, control, and estimation for aerial robots tethered by cables or bars. *IEEE Transactions on Robotics*, 33(4):834–845, 2017.

[80] M. Tognon and A. Franchi. *Theory and Applications for Control of Aerial Robots in Physical Interaction Through Tethers*, volume 140. Springer Tracts in Advanced Robotics, 2020.

[81] S. Park, J. Lee, J. Ahn, M. Kim, J. Her, G. Yang, and D. Lee. Odar: Aerial manipulation platform enabling omnidirectional wrench generation. *IEEE/ASME Transactions on Mechatronics*, 23(4):1907–1918, Aug 2018.

[82] G. Nava, Q. Sablé, M. Tognon, D. Pucci, and A. Franchi. Direct force feedback control and online multi-task optimization for aerial manipulators. *IEEE Robotics and Automation Letters*, 5(2):331–338, 2020.

[83] S. Kim, S. Choi, and H. J. Kim. Aerial manipulation using a quadrotor with a two dof robotic arm. In *2013 IEEE/RSJ International Conference on Intelligent Robots and Systems*, pages 4990–4995, 2013.

[84] Hoseong Seo, Suseong Kim, and H Jin Kim. Aerial grasping of cylindrical object using visual servoing based on stochastic model predictive control. In *2017 IEEE international conference on robotics and automation (ICRA)*, pages 6362–6368. IEEE, 2017.

[85] S. Hamaza, I. Georgilas, M. Fernandez, P. Sanchez, T. Richardson, G. Heredia, and A. Ollero. Sensor installation and retrieval operations using an unmanned aerial manipulator. *IEEE Robotics and Automation Letters*, 4(3):2793–2800, 2019.

[86] K. Bodie, M. Brunner, M. Pantic, S. Walser, P. Pfändler, U. Angst, R. Siegwart, and J. Nieto. Active interaction force control for contact-based inspection with a fully actuated aerial vehicle. *IEEE Transactions on Robotics*, pages 1–14, 2020.

[87] Karen Bodie, Maximilian Brunner, Michael Pantic, Stefan Walser, Patrick Pfändler, Ueli M Angst, Roland Siegwart, and Juan I. Nieto. An omnidirectional aerial manipulation platform for contact-based inspection. In *Proc. of Robotics: Science and Systems (RSS)*, pages 1–9, 2019.

[88] M. Orsag, C. Korpela, S. Bogdan, and P. Oh. Valve turning using a dual-arm aerial manipulator. In *2014 International Conference on Unmanned Aircraft Systems (ICUAS)*, pages 836–841, 2014.

[89] R. Cano, C. Pérez, F. Oliveros Pruaño, A. Ollero, and G. Heredia. Mechanical design of a 6-dof aerial manipulator for assembling bar structures using uavs. In *2nd RED-UAS*, 2014.

[90] K. Steich, M. Kamel, P. Beardsley, M. K. Obrist, R. Siegwart, and T. Lachat. Tree cavity inspection using aerial robots. In *2016 IEEE/RSJ International Conference on Intelligent Robots and Systems (IROS)*, pages 4856–4862. IEEE, 2016.

[91] P. Chermprayong, K. Zhang, F. Xiao, and M. Kovac. An integrated delta manipulator for aerial repair: A new aerial robotic system. *IEEE Robotics Automation Magazine*, 26(1):54–66, 2019.

[92] R. Naldi, A. Macchelli, N. Mimmo, and L. Marconi. Robust control of an aerial manipulator interacting with the environment. *IFAC-PapersOnLine*, 51(13):537–542, 2018.

[93] H. W. Wopereis, J.J. Hoekstra, T.H. Post, G. A Folkertsma, Stefano Stramigioli, and Matteo Fumagalli. Application of substantial and sustained force to vertical surfaces using a quadrotor. In *2017 IEEE international conference on robotics and automation (ICRA)*, pages 2704–2709. IEEE, 2017.

[94] K. Alexis, G. Darivianakis, M. Burri, and R. Siegwart. Aerial robotic contact-based inspection: planning and control. *Autonomous Robots*, 40(4):631–655, 2016.

[95] I. Palunko, P. Cruz, and R. Fierro. Agile load transportation: Safe and efficient load manipulation with aerial robots. *IEEE robotics & automation magazine*, 19(3):69–79, 2012.

[96] I. Palunko, A. Faust, P. Cruz, L. Tapia, and R. Fierro. A reinforcement learning approach towards autonomous suspended load manipulation using aerial robots. In *Robotics and Automation (ICRA), 2013 IEEE International Conference on*, pages 4896–4901. IEEE, 2013.

[97] K. Sreenath, N. Michael, and V. Kumar. Trajectory generation and control of a quadrotor with a cable-suspended load-a differentially-flat hybrid system. In *Robotics and Automation (ICRA), 2013 IEEE International Conference on*, pages 4888–4895. IEEE, 2013.

[98] P. Foehn, D. Falanga, N. Kuppuswamy, R. Tedrake, and D. Scaramuzza. Fast trajectory optimization for agile quadrotor maneuvers with a cable-suspended payload. In *Robotics: Science and Systems*, pages 1–10, 2017.

[99] F. Augugliaro, A. Mirjan, F. Gramazio, M. Kohler, and R. D'Andrea. Building tensile structures with flying machines. In *2013 IEEE/RSJ International Conference on Intelligent Robots and Systems*, pages 3487–3492, 2013.

[100] N. Staub, D. Bicego, Q. Sablé, V. Arellano-Quintana, S. Mishra, and A. Franchi. Towards a flying assistant paradigm: the OTHex. In *2018 Proc. of the IEEE Int. Conf. on Robotics & Automation (ICRA)*, pages 6997–7002, Brisbane, Australia, May 2018.

[101] N. Staub, M. Mohammadi, D. Bicego, Q. Delamare, H. Yang, D. Prattichizzo, P. Robuffo Giordano, D. Lee, and A. Franchi. The tele-magmas: An aerial-ground comanipulator system. *IEEE Robotics Automation Magazine*, 25(4):66–75, Dec 2018.

[102] A. Nikou, G. C. Gavridis, and K. J. Kyriakopoulos. Mechanical design, modelling and control of a novel aerial manipulator. In *2015 Proc. of the IEEE Int. Conf. on Robotics & Automation (ICRA)*, pages 4698–4703, Seattle, WA, USA, may 2015.

[103] C. Papachristos, K. Alexis, and A. Tzes. Dual-authority thrust-vectoring of a tri-tiltrotor employing model predictive control. *Journal of Intelligent & Robotic Systems*, 81(3-4):471, 2016.

[104] T. Anzai, M. Zhao, S. Nozawa, F. Shi, K. Okada, and M. Inaba. Aerial grasping based on shape adaptive transformation by halo: horizontal plane transformable aerial robot with closed-loop multilinks structure. In *IEEE International Conference on Robotics and Automation*, 2018.

[105] M. Zhao, K. Kawasaki, X. Chen, S. Noda, K. Okada, and M. Inaba. Whole-body aerial manipulation by transformable multirotor with two-dimensional multilinks. In *2017 IEEE International Conference on Robotics and Automation (ICRA)*, pages 5175–5182, 2017.

[106] M. Zhao, F. Shi, T. Anzai, K. Okada, and M. Inaba. Online motion planning for deforming maneuvering and manipulation by multilinked aerial robot based on differential kinematics. *IEEE Robotics and Automation Letters*, 5(2):1602–1609, 2020.

[107] R. Naldi, A. Ricco, A. Serrani, and L. Marconi. A modular aerial vehicle with redundant actuation. In *International Conference on Intelligent Robots and Systems*, pages 1393–1398, 2013.

[108] D. Sanalitro, H. J. Savino, M. Tognon, J. Cortés, and A. Franchi. Full-pose manipulation control of a cable-suspended load with multiple UAVs under uncertainties. *IEEE Robotics and Automation Letters*, 5(2):2185–2191, 2020.

[109] H. Yang, S. Park, J. Lee, J. Ahn, D. Son, and D. Lee. Lasdra: Large-size aerial skeleton system with distributed rotor actuation. In *2018 IEEE International Conference on Robotics and Automation (ICRA)*, pages 7017–7023, May 2018.

[110] C. Korpela, P. Brahmbhatt, M. Orsag, and P. Oh. Towards the realization of mobile manipulating unmanned aerial vehicles (mm-uav): Peg-in-hole insertion tasks. In *2013 IEEE Conference on Technologies for Practical Robot Applications (TePRA)*, pages 1–6, April 2013.

[111] Y. Sarkisov, M. J. Kim, D. Bicego, D. Tsetserukou, C. Ott, A. Franchi, and K. Kondak. Development of SAM: cable-suspended aerial manipulator. In *2019 Proc. of the IEEE Int. Conf. on Robotics & Automation (ICRA)*, Montreal, Canada, May 2019.

[112] G. Garimella and M. Kobilarov. Towards model-predictive control for aerial pick-and-place. In *2015 IEEE International Conference on Robotics and Automation (ICRA)*, pages 4692–4697, 2015.

[113] T. Bartelds, A. Capra, S. Hamaza, S. Stramigioli, and M. Fumagalli. Compliant aerial manipulators: Toward a new generation of aerial robotic workers. *IEEE Robotics and Automation Letters*, 1(1):477–483, 2016.

[114] S. Kim, H. Seo, and H. J. Kim. Operating an unknown drawer using an aerial manipulator. In *2015 IEEE International Conference on Robotics and Automation (ICRA)*, pages 5503–5508, 2015.

[115] D. Falanga, K. Kleber, S. Mintchev, D. Floreano, and D. Scaramuzza. The foldable drone: A morphing quadrotor that can squeeze and fly. *IEEE Robotics and Automation Letters*, 4(2):209–216, 2019.

[116] M. Zhao, F. Shi, T. Anzai, K. Chaudhary, X. Chen, K. Okada, and M. Inaba. Flight motion of passing through small opening by dragon: Transformable multilinked aerial robot. In *Int. Conference on Intelligent Robots and Systems (IROS)*, pages 4735–4742, 2018.

[117] T. Anzai, M. Zhao, M. Murooka, F. Shi, K. Okada, and M. Inaba. Design, modeling and control of fully actuated 2d transformable aerial robot with 1 dof thrust vectorable link module. In *2019 IEEE/RSJ International Conference on Intelligent Robots and Systems (IROS)*, pages 2820–2826, 2019.

[118] B. Yüksel, S. Mahboubi, C. Secchi, H. H. Bülthoff, and A. Franchi. Design, identification and experimental testing of a light-weight flexible-joint arm for aerial physical interaction. In *2015 IEEE International Conference on Robotics and Automation (ICRA)*, pages 870–876, 2015.

[119] C. D. Bellicoso, L. R. Buonocore, V. Lippiello, and B. Siciliano. Design, modeling and control of a 5-dof light-weight robot arm for aerial manipulation. In *2015 23rd Mediterranean Conference on Control and Automation (MED)*, pages 853–858, 2015.

[120] A. Suarez, A. E. Jimenez-Cano, V. Manuel Vega, G. Heredia, A. Rodriguez-Castaño, and A. Ollero. Design of a lightweight dual arm system for aerial manipulation. *Mechatronics*, 50:30 – 44, 2018.

[121] A. Suarez, P. Sanchez-Cuevas, M. Fernandez, M. Perez, G. Heredia, and A. Ollero. Lightweight and compliant long reach aerial manipulator for inspection operations. In *2018 IEEE/RSJ International Conference on Intelligent Robots and Systems (IROS)*, pages 6746–6752, 2018.

[122] F. Ruggiero, M. A. Trujillo, R. Cano, H. Ascorbe, A. Viguria, C. Peréz, V. Lippiello, A. Ollero, and B. Siciliano. A multilayer control for multirotor UAVs equipped with a servo robot arm. In *2015 Proc. of the IEEE Int. Conf. on Robotics & Automation (ICRA)*, pages 4014–4020, Seattle, WA, May 2015.

[123] A. Suarez, G. Heredia, and A. Ollero. Lightweight compliant arm with compliant finger for aerial manipulation and inspection. In *2016 IEEE/RSJ International Conference on Intelligent Robots and Systems (IROS)*, pages 4449–4454. IEEE, 2016.

[124] A Suarez, AM Giordano, K. Kondak, G. Heredia, and A. Ollero. Flexible link long reach manipulator with lightweight dual arm: Soft-collision detection, reaction, and obstacle localization. In *Int. Conference on Soft Robotics (RoboSoft)*, pages 406–411, 2018.

[125] A. Suarez, G. Heredia, and A. Ollero. Lightweight compliant arm for aerial manipulation. In *2015 IEEE/RSJ International Conference on Intelligent Robots and Systems (IROS)*, pages 1627–1632. IEEE, 2015.

[126] A. Y. Mersha, S. Stramigioli, and R. Carloni. On bilateral teleoperation of aerial robots. *IEEE Transactions on Robotics*, 30(1):258–274, 2014.

[127] M. Tognon, B. Yüksel, G. Buondonno, and A. Franchi. Dynamic decentralized control for protocentric aerial manipulators. In *2017 Proc. of the IEEE Int. Conf. on Robotics & Automation (ICRA)*, pages 6375–6380, Singapore, May 2017.

[128] S. Kim, H. Seo, and J. Shin H. J. Kim. Cooperative aerial manipulation using multirotors with multi-dof robotic arms. *IEEE/ASME Transactions on Mechatronics*, 23(2):702–713, 2018.

[129] D. Melinger, M. Shomin, and V. Kumar. Cooperative grasping and transport using multiple quadrotors. In *International Symposium on Distributed Autonomous Robots*, 2010.

[130] H. Nguyen, S. Park, J. Park, and D. Lee. A novel robotic platform for aerial manipulation using quadrotors as rotating thrust generators. *IEEE Transactions on Robotics*, 34(2):353–369, April 2018.

[131] R. Ritz and R. D'Andrea. Carrying a flexible payload with multiple flying vehicles. In *IEEE/RSJ International Conference on Intelligent Robots and Systems*, pages 3465–3471, 2013.

[132] H. Yang, M. S. Kim, and D. J. Lee. Distributed rotor-based vibration suppression for flexible object transport and manipulation. In *IEEE International Conference on Robotics and Automation*, 2020.

[133] Koushil Sreenath and Vijay Kumar. Dynamics, control and planning for cooperative manipulation of payloads suspended by cables from multiple quadrotor robots. In *Robotics: Science and Systems*, 2013.

[134] M. Gassner, T. Cieslewski, and D. Scaramuzza. Dynamic collaboration without communication: Vision-based cable-suspended load transport with two quadrotors. In *IEEE International Conference on Robotics and Automation*, pages 5196–5202, 2017.

[135] A. Tagliabue, M. Kamel, R. Siegwart, and J. Nieto. Robust collaborative object transportation using multiple mavs. *International Journal of Robotics Research*, 38(9):1020–1044, 2019.

[136] H. Yang and D. J. Lee. Hierarchical cooperative control framework of multiple quadrotor-manipulator systems. In *IEEE International Conference on Robotics and Automation*, pages 4656–4662, 2015.

[137] F. Caccavale, G. Giglio, G. Muscio, and F. Pierri. Cooperative impedance control for multiple uavs with a robotic arm. In *IEEE/RSJ International Conference on Intelligent Robots and Systems*, pages 2366–2371, 2015.

[138] H. Lee, H. Kim, and H. J. Kim. Path planning and control of multiple aerial manipulators for a cooperative transportation. In *IEEE/RSJ International Conference on Intelligent Robots and Systems*, 2015.

[139] S. Kim, H. Seo, and J. Shin H. J. Kim. Cooperative in the air: a learning-based approach for the efficient motion planning of aerial manipulators. *IEEE Robotics and Automation Magazine*, 25(4):76–85, 2018.

[140] G. Loianno and V. Kumar. Cooperative transportation using small quadrotors using monocular vision and inertial sensing. *IEEE Robotics and Automation Letters*, 3(2):680–687, 2018.

[141] H-N. Nguyen, S. Park, and D. J. Lee. Aerial tool operation system using quadrotors as rotating thrust generators. In *IEEE/RSJ International Conference on Intelligent Robots and Systems*, 2015.

[142] M. Mohammadi, A. Franchi, D. Barcelli, and D. Prattichizzo. Cooperative aerial tele-manipulation with haptic feedback. In *2016 IEEE/RSJ International Conference on Intelligent Robots and Systems (IROS)*, pages 5092–5098, Oct 2016.

[143] T. W. Nguyen, L. Catoire, and E. Garone. Control of a quadrotor and a groud vehicle manipulating an object. *Automatica*, 105:384–390, 2019.

[144] N. Staub, M. Mohammadi, D. Bicego, D. Prattichizzo, and A. Franchi. Towards robotic MAGMaS: Multiple aerial-ground manipulator systems. In *2017 Proc. of the IEEE Int. Conf. on Robotics & Automation (ICRA)*, Singapore, May 2017.

[145] H. Yang, N. Staub, A. Franchi, and D. J. Lee. Modeling and control of multiple aerial-ground manipulator system (magmas) with load flexibility. In *IEEE/RSJ International Conference on Intelligent Robots and Systems*, 2018.

[146] B. Gabrich, D. Saldana, V. Kumar, and M. Yim. A flying gripper based on cuboid modular robots. In *IEEE International Conference on Robotics and Automation*, 2018.

[147] R. Oung, F. Bourgault, M. Donovan, and R. D'Andrea. The distributed flight array. In *IEEE International Conference on Robotics and Automation*, pages 601–607, 2010.

[148] M. Zhao, T. Anzai, F. Shi, X. Chen, K. Okada, and M. Inaba. Design, modeling, and control of an aerial robot dragon: a dual-rotor-embedded multilink robot with the ability of multi-degree-of-freedom aerial transformation. *IEEE Robotics and Automation Letters*, 3(2):1176–1183, 2018.

[149] S. Park, Y. Lee, J. Heo, and D. Lee. Pose and posture estimation of aerial skeleton systems for outdoor flying. In *International Conference on Robotics and Automation (ICRA)*, pages 704–710, 2019.

[150] F. Shi, M. Zhao, M. Murooka, K. Okada, and M. Inaba. Aerial regrasping: Pivoting with transformable multilink aerial robot. In *2020 IEEE International Conference on Robotics and Automation (ICRA)*, pages 200–207, 2020.

[151] M. Zhao, K. Kawasaki, T. Anzai, X. Chen, S. Noda, F. Shi, K. Okada, and M. Inaba. Transformable multirotor with two-dimensional multi-links: modeling, control, and whole-body aerial manipulation. *International Journal of Robotics Research*, 37(9):1085–1112, 2018.

[152] T. Anzai, M. Zhao, X. Chen, F. Shi, K. Kawasaki, K. Okada, and M. Inaba. Multilinked multirotor with internal communication system for multiple objects transportation based on form optimization method. In *IEEE/RSJ International Conference on Intelligent Robots and Systems*, pages 5977–5984, 2017.

[153] C. Masone, M. Mohammadi, P. Robuffo Giordano, and A. Franchi. Shared planning and control for mobile robots with integral haptic feedback. *The International Journal of Robotics Research*, 37(11):1395–1420, 2018.

[154] G. Gioioso, M. Mohammadi, A. Franchi, and D. Prattichizzo. A force-based bilateral teleoperation framework for aerial robots in contact with the environment. In *2015 Proc. of the IEEE Int. Conf. on Robotics & Automation (ICRA)*, pages 318–324, Seattle, WA, May 2015.

[155] J. Lee, R. Balachandran, Y. S. Sarkisov, M. De Stefano, A. Coelho, K. Shinde, M. J. Kim, R. Triebel, and K. Kondak. Visual-inertial telepresence for aerial manipulation. *arXiv preprint arXiv:2003.11509*, 2020.

[156] G. Gioioso, A. Franchi, G. Salvietti, S. Scheggi, and D. Prattichizzo. The Flying Hand: a formation of UAVs for cooperative aerial tele-manipulation. In *2014 Proc. of the IEEE Int. Conf. on Robotics & Automation (ICRA)*, pages 4335–4341, Hong Kong, China, May. 2014.

[157] M. De Stefano, R. Balachandran, J. Artigas, and C. Secchi. Reproducing physical dynamics with hardware-in-the-loop simulators: A passive and explicit discrete integrator. In *2017 IEEE International Conference on Robotics and Automation (ICRA)*, pages 5899–5906, 2017.

[158] G. A. Yashin, D. Trinitatova, R. T. Agishev, R. Ibrahimov, and D. Tsetserukou. Aerovr: Virtual reality-based teleoperation with tactile feedback for aerial manipulation. In *2019 19th International Conference on Advanced Robotics (ICAR)*, pages 767–772. IEEE, 2019.

[159] Y. Wu, J. Song, J. Sun, F. Zhu, and H. Chen. Aerial grasping based on vr perception and haptic control. In *2018 IEEE International Conference on Real-time Computing and Robotics (RCAR)*, pages 556–562. IEEE, 2018.

[160] A. Santamaria-Navarro, G. Loianno, J. Solà, V. Kumar, and J. Andrade Cetto. Autonomous navigation of micro aerial vehicles using high-rate and low-cost sensors. *Autonomous Robots*, 42, 12 2017.

[161] W. Martens, Y. Poffet, P. R. Soria, R. Fitch, and S. Sukkarieh. Geometric priors for gaussian process implicit surfaces. *IEEE Robotics and Automation Letters*, 2(2):373–380, April 2017.

[162] C. Kanellakis and G. Nikolakopoulos. Guidance for autonomous aerial manipulator using stereo vision. *Journal of Intelligent & Robotic Systems*, 08 2019.

[163] S. Kim, H. Seo, S. Choi, and H. J. Kim. Vision-guided aerial manipulation using a multirotor with a robotic arm. *IEEE/ASME Transactions on Mechatronics*, 21(4):1912–1923, 2016.

[164] L. De Silva, M. Gharbi, A. K. Pandey, and R. Alami. A new approach to combined symbolic-geometric backtracking in the context of human–robot interaction. In *IEEE international conference on robotics and automation (ICRA)*, 2014.

[165] H. Lv and C. Lu. An assembly sequence planning approach with a discrete particle swarm optimization algorithm. *International Journal of Advanced Manufacturing Technology*, 50(5):761–770, Sept 2010.

[166] G. Tian, M. Zhou, and J. Chu. A chance constrained programming approach to determine the optimal disassembly sequence. *IEEE Transactions on Automation Science and Engineering*, 10(4):1004–1013, Oct 2013.

[167] A. Boeuf, J. Cortés, R. Alami, and T. Siméon. Enhancing sampling-based kinodynamic motion planning for quadrotors. *2015 IEEE/RSJ International Conference on Intelligent Robots and Systems (IROS)*, pages 2447–2452, 2015.

[168] M. Tognon, E. Cataldi, H. A. T. Chavez, G. Antonelli, J. Cortés, and A. Franchi. Control-aware motion planning for task-constrained aerial manipulation. *IEEE Robotics and Automation Letters*, 3(3):2478–2484, 2018.

[169] A. Caballero, M.l Bejar, A. Rodriguez-Castaño, and A. Ollero. Motion planning with dynamics awareness for long reach manipulation in aerial robotic systems with two arms. *International Journal of Advanced Robotic Systems*, 15(3):1729881418770525, 2018.

[170] J. Thomas, J. Polin, K. Sreenath, and V. Kumar. Avian-inspired grasping for quadrotor micro uavs. In *ASME 2013 international design engineering technical conferences and computers and information in engineering conference*. American Society of Mechanical Engineers Digital Collection, 2013.

[171] P. Hannibal, O. Koji, L. Robert, and S. Kazuhiro. A multirotor platform employing a three-axis vertical articulated robotic arm for aerial manipulation tasks. In *2018 IEEE/ASME International Conference on Advanced Intelligent Mechatronics (AIM)*, pages 478–485. IEEE, 2018.

[172] H. W. Wopereis, T. D. van der Molen, T. H. Post, S. Stramigioli, and M. Fumagalli. Mechanism for perching on smooth surfaces using aerial impacts. In *2016 IEEE International Symposium on Safety, Security, and Rescue Robotics (SSRR)*, pages 154–159, 2016.

[173] A. López-Lora, P. J. Sánchez-Cuevas, A. Garofano, A. Suárez, A. Ollero, and G. Heredia. Mhyro: Modular hybrid robot for contact inspection and maintenance in oil and gas plants. In *2020 Proc. of the IEEE/RSJ Int. Conf. on Intelligent Robots and Systems (IROS)*. IEEE, 2020.

[174] Adnan S. Saeed, Ahmad Bani Younes, Chenxiao Cai, and Guowei Cai. A survey of hybrid unmanned aerial vehicles. *Progress in Aerospace Sciences*, 98:91 – 105, 2018.

[175] C. Papachristos, K. Alexis, and A. Tzes. Design and experimental attitude control of an unmanned tilt-rotor aerial vehicle. In *Intl. Conf. on Advanced Robotics*, pages 465–470, 2011.

[176] S. Verling, T. Stastny, G. Bättig, K. Alexis, and R. Siegwart. Model-based transition optimization for a vtol tailsitter. In *2017 IEEE International Conference on Robotics and Automation (ICRA)*, pages 3939–3944, May 2017.

[177] S. Mintchev and D. Floreano. Adaptive morphology: A design principle for multimodal and multifunctional robots. *IEEE Robotics Automation Magazine*, 23(3):42–54, Sep. 2016.

[178] S.A. Ansari, R. Żbikowski, and K. Knowles. Aerodynamic modelling of insect-like flapping flight for micro air vehicles. *Progress in Aerospace Sciences*, 42(2):129 – 172, 2006.

[179] M. I. Woods, J. F. Henderson, and G. D. Lock. Energy requirements for the flight of micro air vehicles. *Aeronautical Journal*, 105(1045):135–149, 2001. ID number: ISI:000167498300004.

[180] G. Sachs. New model of flap-gliding flight. *Journal of Theoretical Biology*, 377:110 – 116, 2015.

[181] M. Tognon, R. Alami, and B. Siciliano. Physical human-robot interaction with a tethered aerial vehicle: Application to a force-based human guiding problem. *IEEE Transactions on Robotics*, pages 1–12, 2021.

[182] A. Tagliabue, A. Paris, S. Kim, R. Kubicek, S. Bergbreiter, and J. P. How. Touch the wind: Simultaneous airflow, drag and interaction sensing on a multirotor. In *2020 IEEE/RSJ International Conference on Intelligent Robots and Systems (IROS)*, pages 1645–1652, 2020.

Dr. Anibal Ollero is a Professor and Head of the GRVC Robotics Laboratory at the ETSI University of Seville, Spain. He received Industrial Engineering and PhD Degree from University of Seville, respectively in 1977 and 1980. His main research interest is in aerial robotics. He is the author of more than 750 papers including about 200 papers in peer-reviewed journals, is the recipient of 25 research awards, and is the Co-chair of the IEEE RAS Technical Committee on Aerial Robotics and Unmanned Aerial Vehicles.

Dr. Marco Tognon (S'15-M'18) is a postdoctoral researcher at ETH Zurich, Switzerland, in the ASL group. He received the Ph.D. degree in Robotics in 2018, from INSA Toulouse, France, developing his thesis at LAAS-CNRS. His thesis has been awarded with three prizes. He received the M.Sc. degree in automation engineering in 2014, from the University of Padua, Italy. His current research interests include robotics, aerial physical interaction, multi-robot systems, and human-robot physical interaction.

Dr. Alejandro Suarez is a postdoctoral researcher at University of Seville, Spain, in the GRVC Robotics Labs. He received the B.S. in telecommunications in 2012, the M.Sc. degree in automation engineering in 2013, and the Ph.D. degree in Robotics in 2019 from the University of Seville, developing his research work in the same group since 2012. His thesis has been awarded with two prizes. His current research interests include robotics, aerial robotic manipulation, robotic arm design, and compliance.

Dr. Dongjnu Lee is a Professor with the Department of Mechanical Engineering at Seoul National University (SNU), Korea. He received the B.S. and M.S. degrees from KAIST, Korea, and the Ph.D. degree in mechanical engineering from University of Minnesota, respectively in 1995, 1997 and 2004. His main research interests are the dynamics and control of robotic and mechatronic systems with emphasis on aerial/mobile robots, teleoperation/haptics, multirobot systems, and industrial control applications.

Dr. Antonio Franchi (S'07-M'11-SM'16) is a Professor of Robotics in the Faculty of Electrical Engineering, Mathematics & Computer Science, at the University of Twente, The Netherlands. His interests are the design and control for robotic systems with applications to multi-robot systems and aerial robots. He co-authored about 140 papers/chapters in peer-reviewed international journals, conferences, books. He is the co-founder and co-chair of the IEEE RAS Technical Committee on Multiple Robot Systems.